DOI: 10.1021/ma101736j

Macromolecules
ARTICLE

Atom Transfer Radical Polymerization of Isobornyl Acrylate: A Kinetic Modeling Study

Dagmar R. D'hooge,[†] Marie-Françoise Reyniers,*[,†] Florian J. Stadler,[‡,§] Bart Dervaux,[⊥] Christian Bailly,[‡] Filip E. Du Prez,[⊥] and Guy B. Marin[†]

[†]*Laboratory for Chemical Technology, Department of Chemical Engineering Ghent University, Krijgslaan 281 (S5), B-9000 Gent, Belgium,* [‡]*Unité de Physique et de Chimie des Hauts Polymères Département des science des matériaux et de procédés Université Catholique de Louvain, Croix du Sud 1, B-1348 Louvain-la-Neuve, Belgium,* [§]*Department of Chemical Engineering, Chonbuk National University, 561-756 Jeonju, South Korea, and* [⊥]*Polymer Chemistry Research Group, Department of Organic Chemistry, Ghent University, Krijgslaan 281 (S4-bis), B-9000 Gent, Belgium*

Received January 7, 2010; Revised Manuscript Received September 24, 2010

ABSTRACT: A detailed kinetic modeling study of the atom transfer radical polymerization (ATRP) of isobornyl acrylate (iBoA) is presented. This study combines a detailed reaction scheme with a systematic approach to account for diffusional limitations. Calculated values for diffusion coefficients and the Williams−Landel−Ferry parameters for poly(iBoA) are based on rheological measurements. A good agreement with experimental data is obtained for the polymerization rate, average chain length, and polydispersity index in conditions ranging from 323 to 348 K for targeted chain lengths varying from 50 to 100 and initial activator/deactivator concentrations between 10−50/0−2.5 mol m^{-3}. In these conditions, βC-scission reactions are insignificant and backbiting reactions result in a slight decrease of the polymerization rate and level of control at high conversions only. Termination is subject to diffusional limitations during the whole ATRP, while diffusional limitations on deactivation cannot be neglected at higher conversion. Diffusional limitations are shown to be codetermined by the evolution of the chain length distribution of both the end-chain and mid-chain macromolecular species.

1. Introduction

Atom transfer radical polymerization (ATRP) belongs to the group of the controlled radical polymerization (CRP) techniques. Via CRP, (block-co)polymers can be synthesized that are characterized by an almost uniform chain length and having end-group functionality.[1] In particular for ATRP, this end-group functionality (X) is usually a halogen atom, which can be easily modified into another functional group.

The reaction mechanism of ATRP is presented in Figure 1. Initiator molecules $R_{ini}X$ are activated into initiating radicals R_{ini} by activator molecules $M_t^nL_yX$. The initiating radicals R_{ini} can propagate, terminate, or undergo chain transfer to monomer as in free radical polymerization (FRP). The (propagating) radicals can, however, also be deactivated leading to the formation of dormant species and thus to reincorporation of the end-group functionality X.

For sufficiently high deactivation rate coefficients, a low radical concentration can be obtained resulting in a limited contribution of termination and chain transfer reactions and, hence, in a restricted loss of polymer end-group functionality. Moreover, if initiation is fast enough, a low value for the polydispersity index of the molar mass distribution (MMD) of the polymer can be obtained.

Kinetic studies on acrylate FRP have indicated that its kinetics can be complicated by the occurrence of intramolecular chain transfer (i.e., backbiting), intermolecular chain transfer, and βC-scission reactions.[2−6] Backbiting and intermolecular chain transfer reactions both result in the formation of less reactive tertiary midchain macroradicals leading to a reduced polymerization rate and to the occurrence of short and long chain branches, respectively. In agreement with earlier findings of Chiefari et al.,[2] Barth et al.[6] have recently shown, using electron paramagnetic resonance (EPR) measurements, that intermolecular chain transfer reactions are of minor importance. βC-scission reactions of mid-chain macroradicals, resulting in the formation of secondary end-chain macroradicals of reduced chain length and macromonomers, are expected to become important only at elevated temperatures,[4] and their occurrence also strongly depends on the monomer and radical concentrations in the system. At 411 K and under starved-feed conditions only, a significant fraction of poly(*n*-butyl acrylate) mid-chain macroradicals were found to undergo βC-scission reactions.[5] Also, Ahmad et al.[7] found no proof of the presence of unsaturations due to βC-scission reactions in their recent ^{13}C nuclear

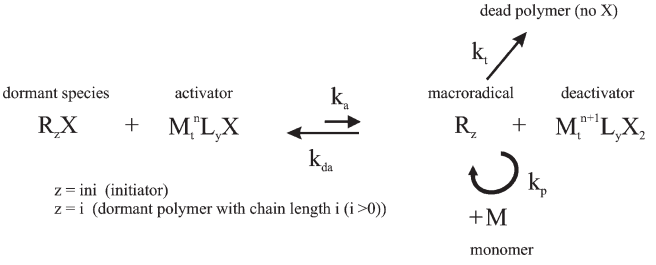

Figure 1. Mechanism of ATRP. k_a, k_{da}, k_p, and k_t: rate coefficient of activation, deactivation, propagation, and termination (m^3 mol^{-1} s^{-1}). $M_t^{n/n+1}$ = transition metal; L = ligand, X = halogen atom, $n(+1)$ = oxidation number; y = number of ligands.

*Corresponding author: e-mail MarieFrancoise.Reyniers@UGent.be; tel 0032 (0)9 2645677; fax 0032 (0)9 2644999.

 Published on Web 10/15/2010

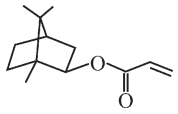

Figure 2. Isobornyl acrylate (iBoA).

magnetic resonance (NMR) spectroscopic study of controlled radical polymerizations with *n*-butylacrylate (*n*-BuA) at 353 K.

Dervaux et al.[8] recently reported the determination of the intrinsic chemical propagation rate coefficient ($k_{p,chem}$) of isobornyl acrylate (iBoA; Figure 2), *tert*-butyl acrylate, and ethoxyethyl acrylate using pulsed laser polymerization (PLP). For iBoA, from 278 to 343 K these authors observed a deviation of less than 5% between $k_{p,chem}$ values based on the two first inflection points of the PLP MMD, suggesting a limited contribution of backbiting in the polymerization of iBoA in the temperature range 278−343 K. On the other hand, for ethoxyethyl acrylate and *tert*-butyl acrylate these authors observed a deviation up to 20%, from respectively 343 and 353 K, onward, indicating a more pronounced importance of backbiting for the polymerization of these monomers as compared to iBoA polymerization.

Very recently, Ahmad et al.[7] have shown, using ^{13}C NMR spectroscopy, that the level of branching in *n*-BuA polymerization is reduced significantly when using CRP as compared to FRP. In particular, in the ATRP of *n*-BuA at 353 K using Cu(I)Br/PMDETA (PMDETA: *N*,*N*,*N*′,*N*″,*N*″-pentamethyldiethylenetriamine) as catalyst and methyl 2-bromo propionate (MBP) as initiator, a branching content of ca. 0.40−0.70 mol % was found at almost complete conversion. In contrast, a branching content of ca. 2 mol % was found in the FRP of *n*-BuA already at a lower temperature of 343 K. These authors also tested several explanations to account for the strikingly different branching levels in polyacrylates by FRP and CRP based on simplified kinetic models and explained the observations in terms of differences in the concentration of highly reactive "short-chain radicals". In FRP, the radical chain length distribution (CLD) is broad, and a significant fraction of "short-chain radicals" is always present, whereas in CRP, the radical CLD is narrow with only a small fraction of "short-chain radicals", which diminishes as polymerization goes on. Hence, CRP gives rise to lower levels of branching, when performed under otherwise similar conditions to FRP.[7] Also, the studied ATRP of *n*BuA resulted in a high level of control: a polydispersity index below 1.2 was obtained, and the increase of the average chain length with conversion was almost identical to the ideal theoretical one, indicative of a reduced importance of mid-chain macroradicals in ATRP. Note that, in view of the different reactivity of the tertiary mid-chain macroradicals as compared to the secondary end-chain macroradicals, the regular ATRP activation−growth−deactivation process can become disturbed due to the gradually increasing importance of backbiting as monomer consumption proceeds and therefore can lead to a decrease in control of the ATRP. Also, simulation of the ATRP of isobornyl acrylate at 343 K reported by Dervaux et al.[9] using an intrinsic kinetic model showed that a significant reduction of the polymerization rate is to be expected only for very high short branching contents, i.e., in case 85% of mid-chain macroradicals are formed from low conversions onward.

The previous findings indicate that side reactions, such as backbiting and βC-scission, can be expected to have a limited influence in the ATRP of iBoA, in particular at low conversions and at temperatures below 343 K. Dervaux et al.[10] have also demonstrated that poly(isobornyl acrylate) (piBoA) can be easily synthesized via ATRP in a controlled manner. Therefore, iBoA is chosen as monomer for a kinetic study aimed at obtaining more insight into the kinetics of the ATRP activation−deactivation process as the hydrophobic piBoA is of interest for the controlled synthesis of amphiphilic copolymers with hydrophilic poly(acrylic acid) segments.[8] Also, in view of its exceptionally high glass transition temperature ($T_{g,p}$ = 367 K[11]), iBoA can be used as an alternative for other polymers that have a similar glass transition temperature but are less easily synthesized in a controlled manner by ATRP, such as poly(methyl methacrylate) ($T_{g,p}$ = 378 K[12]) and polystyrene ($T_{g,p}$ = 373 K[12]). However, most studies on piBoA are limited to qualitative reports on (co)polymerization with iBoA, and only a limited number of research groups have investigated the kinetics of FRP and/or CRP of iBoA.[10,11,13] Also, most of the kinetic modeling studies available in the literature neglect the well-known influence of diffusional limitations on termination and/or deactivation on the kinetics of the polymerization.[14−17]

This work focuses on the kinetics of the activation−deactivation process in the ATRP of iBoA in ethyl acetate with copper bromide as transition metal salt, PMDETA as ligand, and MBP as initiator and on the influence of diffusional limitations on the kinetics of the ATRP. Ethyl acetate is chosen as solvent as it shows a high solubility for both the activator and the deactivator. A detailed reaction network, including backbiting and βC-scission, is used to develop a kinetic model that is able to describe the polymerization rate and the polymer properties accounting for diffusional limitations by an explicit a priori calculation of the diffusion coefficients of the reaction components using the Vrentas and Duda free volume theory.[18,19] In particular the dynamic viscosities of iBoa and piBoA are measured at temperatures ranging from 280 to 350 K and above $T_{g,p}$, respectively, allowing the calculation of the required diffusion coefficients and the Williams−Landel−Ferry (WLF) parameters of piBoA.

2. Experimental Procedure

2.1. Materials. Isobornyl acrylate (iBoA; monomer (M); Aldrich, tech.) was purified by vacuum distillation (394 K/18 mmHg). Copper(I) bromide (Cu(I)Br (M_t^nX); Aldrich; 98% (metal based)) was purified by stirring with acetic acid, then by filtering and washing with methanol, and finally by drying in a vacuum oven at 343 K. *N*,*N*,*N*′,*N*″,*N*″-Pentamethyldiethylenetriamine (PMDETA; ligand (L); Acros; 99+%) was distilled (358−359 K/12 mmHg). Methyl 2-bromopropionate (MBP; initiator ($R_{ini}X = R_0X$); Acros; 99%) and copper(II) bromide (Cu(II)Br_2 ($M_t^{n+1}X_2$); Aldrich, 99% (metal based)) were used as received. Solvents were purchased from Aldrich (HPLC grade) and used without further purification. All other chemicals were also used as received.

2.2. ATRP of Isobornyl Acrylate. Experimental studies[20,21] have indicated that only the soluble fraction of the activator and the deactivator is involved in the activation−deactivation process and that the polarity of the reaction system can have a significant influence on the solubility limits. Fu et al.[21] obtained perfect solubility for the activator and the deactivator in acetonitrile, which is a rather polar solvent, whereas in toluene, which is a rather nonpolar solvent, a low solubility is obtained; solubility limits lower than 50 mol m^{-3} were measured in toluene. As the solvent used in this work, ethyl acetate, is rather polar and no precipitation of the ATRP catalyst has been observed during the ATRP experiments, perfect solubility of the activator and deactivator can be safely assumed for the ATRP catalyst.

An overview of the polymerization conditions investigated is given in Table 1. A typical ATRP experiment (e.g., entry 5 in Table 1) was carried out as follows. First, a mixture of 1.40×10^{-2} mol of iBoA (i.e., 3.00×10^{-6} m^3) and 2.13×10^{-4} mol of PMDETA (i.e., 4.40×10^{-8} m^3) was bubbled with nitrogen for 1 h to remove dissolved oxygen. Analogously, ethyl acetate was bubbled with nitrogen for 1 h, after which 1.50×10^{-6} m^3

Table 1. Overview of Polymerization Conditions Covered in the Experimental Study of the ATRP of iBoA in Ethyl Acetate[a]

entry	T_{pol} (K)	$[iBoA]_0/[MBP]_0$	$([Cu(I)Br]_0 + [Cu(II)Br_2]_0)/[MBP]_0$	$[Cu(II)Br_2]_0/([Cu(I)Br]_0 + [Cu(II)Br_2]_0)$
1	323	100	1.5	0
2	333	100	1.5	0
3	333	100	1.5	0.05
4	333	50	1.5	0
5	343	100	1.5	0
6	343	100	1.5	0.05
7	343	100	0.5	0
8	348	100	1.5	0
9	348	100	0.5	0

[a] For each entry 33 vol % of ethyl acetate with respect to iBoA is used and $([Cu(I)Br]_0 + [Cu(II)Br_2]_0)/[PMDETA]_0 = 1$.

(33 vol % with respect to iBoA) was added to the reaction flask. Subsequently, Cu(I)Br (2.13×10^{-4} mol, 3.00×10^{-2} g) was added under a nitrogen atmosphere, and the reaction flask was placed in an oil bath. As soon as the polymerization temperature (343 K) was obtained, the ATRP was initiated by the addition of MBP (1.58×10^{-8} m^3). At distinct polymerization times, samples were withdrawn from the reaction system to determine the conversion and the polymer properties. Finally, the ATRP was terminated by quenching with liquid nitrogen. After dissolution in tetrahydrofuran (THF), passing over a neutral aluminum oxide column to remove copper and evaporation of the solvent, the polymer was precipitated in a 10-fold excess of methanol.

The conversion profile was measured using gas chromatography (GC), whereas gel permeation chromatography (GPC) was used to obtain the number- and mass-average molar mass of the polymer as a function of conversion and, hence, to calculate the polydispersity index of the MMD of the polymer as a function of conversion. GC analysis was performed on a GC8000 from CE Instruments with a DB-5MS column (60 m $\times$ 2.49×10^{-4} m $\times$ 2.50×10^{-7} m) from J&W Scientific and an autoinjector also from CE Instruments. The detector was a flame ionization detector (FID). The injector and detector temperature were taken equal to 523 K. Initially, the column was run at 323 K for 3 min, followed by heating to 503 K via a constant gradient of 20 K/min and kept at that temperature for 8 min. As internal standard *n*-decane was used. The integration of the detector signal was done with the PeakSimple software package.

GPC analysis was performed on a Waters instrument consisting of three Waters Styragel serial columns (pore sizes: 10^{-7}, 10^{-6}, and 10^{-5} m; particle size: 5×10^{-6} m) at 308 K in combination with a (2410 Waters) refractive index detector. Chloroform was used as eluent at a flow rate of 1.50×10^{-6} m^3/min. The Breeze software of Waters was used for the integration of the detector signals. Triple detection showed a good agreement between the theoretically predicted and the experimentally obtained molar masses for different polymer samples. By means of the same technique, a correction factor of 1.45 was obtained for the conversion of the molar mass data obtained by a polystyrene calibrated GPC system to the "exact" data. It should be noted that such approach is fast and has proven to be successful in polymerization analysis.[22]

Unfortunately, ^{13}C NMR did not allow to quantify the branching content due to overlap with the quaternary isobornyl C atoms.

2.3. Rheological Measurements. The rheological measurements on the polymer were performed using a TA Instruments ARES and a Malvern Gemini, using parallel plate geometries (8.0×10^{-3} m for measurements close to the glass transition temperature of the polymer ($T_{g,p}$) and 25×10^{-3} m for measurements significantly above $T_{g,p}$). The experiments were performed in a nitrogen atmosphere to minimize thermooxidative degradation. Frequency sweeps were carried out every 5−10 K to determine the temperature dependence in the frequency range between $\omega = 0.1$ and 100 s^{-1} using deformations in the linear regime ($\gamma_0 < 50\%$). The thermal expansion of the geometries was also compensated for. All tests were performed several times and averaged to yield maximum reliability.

For the monomer, a Malvern HR nano using a 40.0×10^{-3} m 4° cone−plate geometry and a Peltier oven with solvent trap was used to allow reliable measurement of the low viscosities. As the monomer can considered to be a Newtonian liquid, the temperature dependence was determined from a temperature ramp at a ramp rate of 0.5 K/min to minimize thermal gradients and to allow for long integration times to improve the accuracy. More detailed information about the methods and procedures used for the rheological analysis can be found elsewhere.[23,24]

3. Kinetic Model

Table 2 presents the reactions considered for the ATRP of iBoA in ethyl acetate. A distinction can be made between ATRP specific and ATRP nonspecific reactions steps. Intramolecular chain transfer (i.e., backbiting (*bb*,*e*)) and βC-scission reactions ($\beta C1/2$, *m*) have been taken up in the kinetic model while intermolecular chain-transfer reactions have been neglected based on the recent EPR study of Barth et al.[6] These authors showed that the importance of intermolecular chain-transfer reactions is very low. Termination by disproportionation and chain transfer to monomer reactions are also neglected based on literature data for other acrylate polymerizations.[3]

It can be seen in Table 2 that backbiting reactions result in the formation of tertiary mid-chain macroradicals (indicated by the subscript *m*) which can lead to short-chain branching if these reactions are followed by propagation or termination. Propagation of mid-chain macroradicals results again in the formation of secondary end-chain macroradicals (indicated by the subscript *e*) while βC-scission leads to the formation of end-chain macroradicals having a reduced chain length and macromonomers. Note that for end-chain macroradicals with $i < 3$ backbiting is not considered, as this would imply a branching point in the initiator part, which is very unlikely as pointed out by Ahmad et al.[7]

A distinction is also made between termination by recombination of end-chain macroradicals (*tc*, *ee*) and mid-chain macroradicals (*tc*, *mm*) and their cross-termination (*tc*, *em*). Note that termination reactions involving initiator radicals are considered explicitly in the kinetic model avoiding the need of the explicit introduction of an initiator efficiency in the kinetic model. Simulation results show that, in the conditions used in this work, termination reactions involving initiator radicals are of minor importance resulting in an initiator efficiency close to one.

For each bimolecular reaction *l* in Table 2 ($l = p, tc, a,$ and *da*), diffusional limitations are taken into account via[17,25,26]

$$\frac{1}{k_{l,\mathrm{app}}} = \frac{1}{k_{l,\mathrm{diff}}} + \frac{1}{k_{l,\mathrm{chem}}} \tag{1}$$

in which $k_{l,app}$, $k_{l,diff}$, and $k_{l,chem}$ are respectively the apparent, diffusional, and intrinsic chemical rate coefficient. For the calculation of $k_{l,diff}$, the Smoluchowski model (eq 2[27,28]) is used:

$$k_{l,\mathrm{diff}} = 4\pi N_A \sigma D_{AB} \tag{2}$$

in which N_A is the Avogrado constant and σ and D_{AB} are the collision radius (see section 1 of the Supporting Information[29]) and the mutual diffusion coefficient of the reactants A and B, which is strongly influenced by the dynamic viscosity of the monomer and the polymer.

The intrinsic chemical rate coefficient of each reaction step *l* ($k_{l,chem}$) is calculated by an Arrhenius equation, the parameters of which are listed in Table 2. In this table also the thermodynamic parameters related to the activation−deactivation process are given. As shown

Table 2. Reaction Steps for the ATRP of iBoA and Their Arrhenius/Thermodynamic Parameters for the Calculation of $k_{l,\mathrm{chem}}$ (i, j, q = Chain Length ($i, j \geq 0/3$ (e/m; e/m Related to End-/Mid-Chain Macromolecular Species) with $i = 0$ Related to Reaction with Initiator or Initiating Radical; $q \geq 2$ (Macromonomer)); $k_{l,\mathrm{app}}$ Calculated with eq 1 (l = a, da, p, and tc); for $i = j = 0$, R_0R_0 Is Used Instead of P_0; Only Mid-Chain Macroradicals by Intramolecular Chain Transfer Are Formed ($k^i_{\beta C1/2,m,\mathrm{app}} = 0$ for $i < 4$))

reaction step (l)		$k_{l,\mathrm{chem}}$ [a]
propagation		
(p, e)	$R_{i,e} + M \xrightarrow{k^i_{p,e,\mathrm{app}}} R_{i+1,e}$	$1.1 \times 10^4 \exp\left(-\frac{17000}{RT}\right)$ [b]
(p, m)	$R_{i,m} + M \xrightarrow{k^i_{p,m,\mathrm{app}}} R_{i+1,e}$	$1.5 \times 10^3 \exp\left(-\frac{28900}{RT}\right)$ [b]
(pm, e)	$R_{i,e} + M_q \xrightarrow{k^{i,q}_{p,e,\mathrm{app}}} R_{i+q,m}$	$1.1 \times 10^4 \exp\left(-\frac{17000}{RT}\right))$ [b]
(pm, m)	$R_{i,m} + M_q \xrightarrow{k^{i,q}_{p,m,\mathrm{app}}} R_{i+q,m}$	$1.5 \times 10^3 \exp\left(-\frac{28900}{RT}\right)$ [b]
termination		
(tc, ee)	$R_{i,e} + R_{j,e} \xrightarrow{k^{ij}_{tc,ee,\mathrm{app}}} P_{i+j}$	1.4×10^7 [c]
(tc, em)	$R_{i,e} + R_{j,m} \xrightarrow{k^{ij}_{tc,em,\mathrm{app}}} P_{i+j}$	1.4×10^6 [d]
(tc, mm)	$R_{i,m} + R_{j,m} \xrightarrow{k^{ij}_{tc,mm,\mathrm{app}}} P_{i+j}$	1.4×10^5 [d]
activation		
(a, e)	$R_{i,e}X + M^n_tL_yX \xrightarrow{k^i_{a,e,\mathrm{app}}} R_{i,e} + M^{n+1}_tL_yX_2$	$1.5 \times 10 \exp\left(-\frac{32600}{RT}\right)$ [c]
(a, m)	$R_{i,m}X + M^n_tL_yX \xrightarrow{k^i_{a,m,\mathrm{app}}} R_{i,m} + M^{n+1}_tL_yX_2$	$4.5 \exp\left(-\frac{27500}{RT}\right)$ [e]
deactivation		
(da, e)	$R_{i,e} + M^{n+1}_tL_yX_2 \xrightarrow{k^i_{da,e,\mathrm{app}}} R_{i,e}X + M^n_tL_yX$	$\frac{k^i_{a,e,\mathrm{chem}}}{K^i_{eq,e}}$ [f]
(da, m)	$R_{i,m} + M^{n+1}_tL_yX_2 \xrightarrow{k^i_{da,m,\mathrm{app}}} R_{i,m}X + M^n_tL_yX$	$k^i_{da,e,\mathrm{chem}}$ [g]
backbiting		
(bb, e)	$R_{i,e} \xrightarrow{k^i_{bb,e,\mathrm{chem}}} R_{i,m}$	$1.1 \times 10^4 \exp\left(-\frac{31700}{RT}\right)$ [h]
βC-scission		
($\beta C1$, m)	$R_{i,m} \xrightarrow{k^i_{\beta C1,m,\mathrm{app}}} R_{2,e} + M_{i-2}$	$7 \times 10^9 \exp\left(-\frac{71500}{RT}\right)$ [i]
($\beta C2$, m)	$R_{i,m} \xrightarrow{k^i_{\beta C2,m,\mathrm{app}}} R_{i-3,e} + M_3$	$7 \times 10^9 \exp\left(-\frac{71500}{RT}\right)$ [i]

[a] Units: $m^3\ mol^{-1}\ s^{-1}$ except (bb,e) and ($\beta C1/2$,e) s^{-1}. [b] e: PLP study of iBoA[8] and m: activation energy n-BuA[40] with pre-exponential factor: this work; macromonomer: equal to monomer. [c] This work. [d] Recombination; $k^{ij}_{tc,em,\mathrm{chem}} = k^{ij}_{tc,ee,\mathrm{chem}}/10$ and $k^{ij}_{tc,mm,\mathrm{chem}} = k^{ij}_{tc,ee,\mathrm{chem}}/100$[40] ($n$-BuA); activation energy: 0 J mol^{-1}. [e] Activation energy: activation of EBiB in acetonitrile[32] with pre-exponential factor: this work. [f] $K^i_{eq,e} = \exp(-(\Delta_{r,a,e}H^0 - T\Delta_{r,a,e}S^0)/(RT)) = \exp(-(32500 + T76.9)/(RT))$ (−); this work. [g] $k^i_{da,m,\mathrm{app}} = k^i_{da,e,\mathrm{app}}$. [h] Activation energy: n-BuA polymerization[40] with pre-exponential factor: this work. [i] Activation energy: methyl acrylate trimer polymerization[41] with at 411 K: 12 s^{-1}: n-BuA polymerization[5] and with pre-exponential factor divided by 2 as 2 possibilities.

later (see section 4.2.2), using the Arrhenius and thermodynamic parameters mentioned in Table 2, the observed experimental trends for conversion, average chain length, and polydispersity are captured reasonably well, and the simulated short-chain branching content at temperatures above 348 K and high conversions is found to be similar to the branching content measured by Ahmad et al.[7] in the ATRP of n-BuA using the same catalyst (Cu(I)BrPMDETA) at 353 K at almost complete conversion.

In this work, the chain length dependency of the intrinsic chemical rate coefficients is neglected. It can be expected that this assumption has only a limited effect on the kinetic modeling results, as it is known that the chain length dependent character of $k_{l,\mathrm{chem}}$ is only important at very low chain lengths and for reaction steps on which the effect of diffusional limitations is limited.[30,31] From simulations, it is found that this assumption is indeed valid for the present kinetic modeling study. In particular, for backbiting it will be shown that the chain length distribution of end-chain and mid-chain macroradicals is predominantly determined by the higher chain lengths for which a chain length independent intrinsic chemical rate coefficient can be assumed.[7] Also, no distinction is been made between the intrinsic chemical rate coefficients of initiator molecules and macromolecules. Simulations indicate that, in the conditions used in this work, variation of the intrinsic kinetic parameters for activation/deactivation for initiator/initiator radicals within the typical range reported in the literature has only a minor influence on the conversion, the average chain length, and the polydispersity index profile.

For the propagation of end-chain (macro)radicals, the Arrhenius parameters recently reported by Dervaux et al.[8] are used. These Arrhenius parameters were obtained in the temperature range 273−343 K using pulsed laser polymerization (PLP) without any significant interference of transfer reactions involving mid-chain macroradicals.

For the other reaction steps involved in the ATRP of iBoA, to the best of our knowlegde, no Arrhenius parameters are available in the literature. For acrylate polymerizations, mainly only for reactions involved in the FRP of n-BuA Arrhenius parameters have been reported. It should be noted that for the ATRP-specific reactions almost no data are available in the literature; only for the activation of the commonly available initiators in acetonitrile Arrhenius parameters have been recently reported.[32]

Hence, the simultaneous determination of all remaining Arrhenius parameters appears to be, at first sight, a demanding task. However, since no significant influence of transfer reactions on the polymerization kinetics up to 343 K was observed in the PLP study of iBoA,[8] the importance of mid-chain macroradicals can expected to be limited in the studied ATRP system. Also, on the basis of the experimental study of Ahmad et al.,[7] a very low level of short-chain branching can be expected at low to intermediate conversions in the investigated temperature range. Simulations indicate that that low branching levels at the latter conversions can only be obtained if end-chain macroradicals are dominant up to conversions of ca. 0.40. In a first approximation, it can thus be assumed that at temperatures up to 333 K and at low conversions

Table 3. Continuity Equations of the Reaction Components for the ATRP of iBoA with Backbiting (Part 1; Part 2 in Table 4; i, j, q = Chain Length ($i, j \geq 0$/3 (e/m; End-/Mid-Chain Macromolecular Species) with $i = 0$ Related to Reaction with Initiator or Initiating Radical; $q \geq 2$); $k^{ii}_{tc,ee,\mathrm{app}}$ and $k^{ii}_{tc,mm,\mathrm{app}}$ with Factor 2^{17} Included; $k_{bb,e,\mathrm{chem}} = 0$ and $k^{i}_{p,m,\mathrm{app}} = 0$ for $i < 3$; $\delta(i) = 1$ for $i = 0$; Otherwise 0)

activator

$$\frac{\mathrm{d}M_t^n L_y X}{\mathrm{d}t} = \sum_{j=0}^{\infty} k^{j}_{da,e,\mathrm{app}} R_{e,j} M_t^{n+1} L_y X_2 - \sum_{j=0}^{\infty} k^{j}_{a,e,\mathrm{app}} R_{j,e} X M_t^n L_y X + \sum_{j=3}^{\infty} k^{j}_{da,m,\mathrm{app}} R_{j,m} M_t^{n+1} L_y X_2 - \sum_{j=3}^{\infty} k^{j}_{a,m,\mathrm{app}} R_{j,m} X M_t^n L_y X - \frac{M_t^n L_y X}{V}\frac{\mathrm{d}V}{\mathrm{d}t}$$

deactivator

$$\frac{\mathrm{d}M_t^{n+1} L_y X_2}{\mathrm{d}t} = \sum_{j=0}^{\infty} k^{j}_{a,e,\mathrm{app}} R_{e,j} X M_t^n L_y X - \sum_{j=0}^{\infty} k^{j}_{da,e,\mathrm{app}} R_{j,e} M_t^{n+1} L_y X_2 + \sum_{j=3}^{\infty} k^{j}_{a,m,\mathrm{app}} R_{j,m} X M_t^n L_y X - \sum_{j=3}^{\infty} k^{j}_{da,m,\mathrm{app}} R_{j,m} M_t^{n+1} L_y X_2 - \frac{M_t^{n+1} L_y X_2}{V}\frac{\mathrm{d}V}{\mathrm{d}t}$$

initiating radical ($i = 0$)

$$\frac{\mathrm{d}R_{e,0}}{\mathrm{d}t} = k^{0}_{a,e,\mathrm{app}} R_{e,0} X M_t^n L_y X - k^{0}_{da,e,\mathrm{app}} R_{e,0} M_t^{n+1} L_y X_2 - 2k^{00}_{tc,ee,\mathrm{app}} R_{e,0}{}^2 - \sum_{j=1}^{\infty} k^{0j}_{tc,ee,\mathrm{app}} R_{e,0} R_{j,e} - \sum_{j=3}^{\infty} k^{0,j}_{tc,em,\mathrm{app}} R_{e,0} R_{j,m} - k^{0}_{p,\mathrm{app}} R_{e,0} M - \frac{R_{e,0}}{V}\frac{\mathrm{d}V}{\mathrm{d}t}$$

macroradical $R_{i,e}$ and $R_{j,m}$ ($i = 1/3, \ldots, \infty$)

$$\frac{\mathrm{d}R_{i,e}}{\mathrm{d}t} = k^{i}_{a,e,\mathrm{app}} R_{i,e} X M_t^n L_y X - k^{i}_{da,e,\mathrm{app}} R_{i,e} M_t^{n+1} L_y X_2 - k^{0i}_{tc,ee,\mathrm{app}} R_{e,0} R_{i,e} - \sum_{j=1}^{\infty} k^{ij}_{tc,ee} R_{i,e} R_{j,e} - \sum_{j=3}^{\infty} k^{ij}_{tc,em} R_{i,e} R_{j,m} - k^{i}_{p,e,\mathrm{app}} R_{i,e} M$$
$$+ k^{i-1}_{p,e,\mathrm{app}} R_{i-1,e} M + k^{i-1}_{p,m,\mathrm{app}} R_{i-1,m} M - k^{i}_{bb,e,\mathrm{chem}} R_{i,e} + \delta(i-2) \sum_{j=4}^{\infty} k^{j}_{\beta C1,m,\mathrm{app}} R_{j,m} + k^{i+3}_{\beta C2,m,\mathrm{app}} R_{i+3,m} - \frac{R_{i,e}}{V}\frac{\mathrm{d}V}{\mathrm{d}t}$$

$$\frac{\mathrm{d}R_{i,m}}{\mathrm{d}t} = -k^{i}_{da,m,\mathrm{app}} R_{i,m} M_t^{n+1} L_y X_2 + k^{i}_{a,m,\mathrm{app}} R_{i,m} X M_t^n L_y X - k^{i}_{p,m,\mathrm{app}} R_{i,m} M - \sum_{j=1}^{\infty} k^{ji}_{tc,em} R_{i,m} R_{j,e} + k^{i}_{bb,e,\mathrm{chem}} R_{i,e} - \sum_{j=3}^{\infty} k^{ij}_{tc,mm} R_{i,m} R_{j,m}$$
$$- k^{0i}_{tc,em,\mathrm{app}} R_{e,0} R_{i,m} - k^{i}_{\beta C1,m,\mathrm{app}} R_{i,m} - k^{i}_{\beta C2,m,\mathrm{app}}, R_{i,m} + \sum_{j=1}^{i-2} k^{j,i-j}_{pm,e,\mathrm{app}} R_{j,e} M_{i-j} + \sum_{j=3}^{i-2} k^{j,i-j}_{pm,m,\mathrm{app}} R_{j,m} M_{i-j} - \frac{R_{i,m}}{V}\frac{\mathrm{d}V}{\mathrm{d}t}$$

the polymerization kinetics are not influenced by the occurrence of backbiting reactions. Therefore, for reactions involving end-chain macroradicals, the kinetic parameters for activation and recombination and the thermodynamic parameters of the activation−deactivation process can be obtained by regression of the polymerization data at 323 and 333 K, i.e., at the lowest temperatures investigated, and at low conversion using a kinetic model in which no tertiary mid-chain macroradical formation is included. For a more detailed description of the regression procedure, the reader is referred to section 2 of the Supporting Information.[33] In a next step, the Arrhenius parameters for reaction steps involving mid-chain macroradicals are determined based on the experimental data at the higher temperatures of 343 and 348 K and literature data of kinetic parameters obtained from FRP and PLP studies mostly with *n*-BuA. Although more straightforward techniques for determining these rate coefficients are available, the values reported in Table 2 can, at least, provide ballpark values. It should be emphasized that using these ballpark values already important insights can be obtained in the acrylate ATRP kinetics.

For activation of end-chain dormant polymer molecules, a pre-exponential factor A_a of 14.5 m^3 mol^{-1} s^{-1} and an activation energy $E_{A,a}$ of 32.6 kJ mol^{-1} are obtained. These Arrhenius parameters are similar to the ones recently reported by Seeliger and Matyjaszewski[32] for activation of the structurally related secondary initiator MBP using Cu(I)BrPMDETA in a more polar solvent, i.e., acetonitrile. The latter authors reported a value of 1.2×10^2 m^3 mol^{-1} s^{-1} for the pre-exponential factor and of 33.2 kJ mol^{-1} for the activation energy. However, the intrinsic rate coefficient for activation obtained in this work is ca. 1 order of magnitude lower than the value reported by Seeliger and Matyjaszewski.[32] This difference can, at least partly, be attributed to the lower polarity of the solvent ethyl acetate[34] and to the more rigid structure of a dormant isobornyl acrylate polymer molecule as compared to MBP. Note that this agreement with literature data also further confirms that the importance of mid-chain macroradical formation is indeed low at 323 and 333 K.

Based on the obtained value of 32.5 kJ mol^{-1} for the standard reaction enthalphy of the activation−deactivation process with end-chain macromolecular species ($\Delta_{r,a,e}H^0$) and −76.9 J mol^{-1} K^{-1} for the standard reaction entropy of the activation−deactivation process with end-chain macromolecular species ($\Delta_{r,a,e}S^0$), a value of 8.2×10^{-10} results for the corresponding equilibrium coefficient $K_{eq,e}$ at 335 K. For the ATRP with other acrylates, similar values have been reported for $K_{eq,e}$.[9,35−37] The value of 35 kJ mol^{-1} for $\Delta_{r,a,e}H^0$ reported by Huang et al.[38] for the ATRP of *n*-BuA with Cu(I)Br/PMDETA as catalyst is also in good agreement with the one obtained in this work.

For termination by recombination with end-chain radicals, the activation energy is not estimated significantly different from zero, as expected based on the relatively low values reported for other acrylates (ca. 5 kJ mol^{-1}).[3,31,39]

As can be expected based on the more rigid structure of piBoA, and as reflected by the significantly higher $T_{g,p}$ of piBoA, end-chain macroradicals formed in iBoA polymerization are found to be characterized by a lower, although still similar, intrinsic chemical rate coefficient for backbiting than those formed in *n*-BuA polymerization. In this work, at 335 K a value of ca. 125 s^{-1} is obtained for the intrinsic chemical rate coefficient of backbiting compared to a value of ca. 550 s^{-1} for *n*-BuA. The activation energy for the backbiting reaction is taken as reported in the literature for *n*-BuA polymerization (31.7 kJ mol^{-1}).[40]

For propagation with mid-chain macroradicals, the activation energy is taken as reported in literature for the propagation of *n*-BuA mid-chain macroradicals (28.9 kJ mol^{-1}).[40] At 343 K propagation with mid-chain macroradicals is some 500 times slower compared to propagation with end-chain macroradicals, consistent with literature data.[40]

The intrinsic chemical rate coefficients for termination involving mid-chain macroradicals are obtained by dividing the obtained one related to termination with end-chain macroradicals by a factor 10 and 100 for respectively cross-termination between mid- and end-chain macroradicals and termination between mid-chain macroradicals, as reported in literature.[40]

For activation of mid-chain dormant polymer molecules, a faster activation is considered compared to activation of end-chain dormant polymer molecules. Recently, Seeliger and Matyjaszewski[32] reported that activation with the tertiary initiator ethyl 2-bromoisobutyrate (EBiB) is faster than the activation with the secondary initiator MBP using Cu(I)BrPMDETA as catalyst in acetonitrile. In this work, the activation energy reported by Seeliger and Matyjaszewski for the activation with EBiB (27.5 kJ mol^{-1}) is used for the activation with mid-chain dormant polymer molecules.

The intrinsic chemical rate coefficients for the βC-scission reactions were obtained from literature data. Recently, Wang et al.[5] obtained a value of 12 s^{-1} at 411 K in *n*-BuA polymerization.

Table 4. Continuity Equations of the Reaction Components for the ATRP of iBoA with Backbiting (Part 2; Part 1 in Table 3; i, j, q = Chain Length ($i, j \geq 0$/3 (e/m; End-/Mid-Chain Macromolecular Species) with $i = 0$ Related to Reaction with Initiator or Initiating Radical; $q \geq 2$); $k^{ij}_{tc,ee,\mathrm{app}}$ and $k^{i}_{tc,mm,\mathrm{app}}$ with Factor 2^{17} Included; $k^{i}_{bb,e,\mathrm{chem}} = 0$ and $k^{j}_{p,m,\mathrm{app}} = 0$ for $i < 3$; $\delta(i) = 1$ for $i = 0$; Otherwise 0)

monomer

$$\frac{\mathrm{d}M}{\mathrm{d}t} = -\sum_{j=0}^{\infty} k^{j}_{p,e,app} R_{j,e} M - \sum_{j=3}^{\infty} k^{j}_{p,m,app} R_{j,m} M - \frac{M}{V}\frac{\mathrm{d}V}{\mathrm{d}t}$$

macromonomer ($q \geq 2$)

$$\frac{\mathrm{d}M_q}{\mathrm{d}t} = -\sum_{j=0}^{\infty} k^{j,q}_{pm,e,app} R_{j,e} M_q - \sum_{j=3}^{\infty} k^{j,q}_{pm,m,app} R_{j,m} M_q + k^{q+2}_{\beta C1,m,app} R_{m,q+2} + \delta(q-3) \sum_{j=4}^{\infty} k^{j}_{\beta C2,m,app} R_{j,m} - \frac{M_q}{V}\frac{\mathrm{d}V}{\mathrm{d}t}$$

dormant polymer $R_{i,e}X$ and $R_{i,m}X$ ($i = 0/3, \ldots, \infty$)

$$\frac{\mathrm{d}R_{i,e}X}{\mathrm{d}t} = k^{i}_{da,e,\mathrm{app}} R_{i,e} M_t^{n+1} L_y X_2 - k^{i}_{a,e,\mathrm{app}} R_{i,e} X M_t^{n} L_y X - \frac{R_{i,e}X}{V}\frac{\mathrm{d}V}{\mathrm{d}t}$$

$$\frac{\mathrm{d}R_{i,m}X}{\mathrm{d}t} = k^{i}_{da,m,\mathrm{app}} R_{i,m} M_t^{n+1} L_y X_2 - k^{i}_{a,m,\mathrm{app}} R_{i,m} X M_t^{n} L_y X - \frac{R_{i,m}X}{V}\frac{\mathrm{d}V}{\mathrm{d}t}$$

dead polymer R_0R_0 and P_i ($i = 1, \ldots, \infty$)

$$\frac{\mathrm{d}R_0R_0}{\mathrm{d}t} = k^{00}_{tc,ee,\mathrm{app}} R_{e,0}{}^2 - \frac{R_0R_0}{V}\frac{\mathrm{d}V}{\mathrm{d}t}$$

$$\frac{\mathrm{d}P_i}{\mathrm{d}t} = \frac{1}{2}\sum_{j=1}^{i-1} k^{j,i-j}_{tc,ee,\mathrm{app}} R_{j,e} R_{e,i-j} + k^{0i}_{tc,ee,\mathrm{app}} R_{e,0} R_{i,e} + \frac{1}{2}\sum_{j=3}^{i-1} k^{j,i-j}_{tc,mm,\mathrm{app}} R_{j,m} R_{i-j,m} + k^{0,i}_{tc,mm,\mathrm{app}} R_{e,0} R_{i,m} + \sum_{j=3}^{i-1} k^{j,i-j}_{tc,em,\mathrm{app}} R_{j,e} R_{i-j,m} - \frac{P_i}{V}\frac{\mathrm{d}V}{\mathrm{d}t}$$

In this work, the Arrhenius parameters for the βC-scission reactions were obtained from this value combined with an activation energy of 71.5 kJ mol^{-1}, as reported by Hirano and Yamada[41] in methyl acrylate trimer polymerization. For propagation with the formed macromonomers, the same intrinsic chemical rate coefficients as for the monomer iBoA are used.

Tables 3 and 4 present the batch continuity equations for all reaction components. A distinction is made between non-macromolecules and macromolecules, on the one hand, and between end- and mid-chain macromolecular species, on the other. For the calculation of the volume of the reaction system, the reader is referred to section 3 of the Supporting Information.

The continuity equations in Tables 3 and 4 are integrated according to the methodology described by D'hooge et al.[17] This methodology is based on the method of moments and accounts for moment averaged apparent rate coefficients, i.e., population-weighted apparent rate coefficients, which are calculated using the quasi-steady-state approximation for the macroradicals at each integration step combined with a convergence test. The methodology was tested successfully for the ATRP of methyl methacrylate, in which no mid-chain macroradicals are involved.[17] In this work, the methodology is extended to account for the formation of mid-chain macroradicals, as explained in section 4 of the Supporting Information.

4. Results and Discussion

In this section, first the determination of the hole free volume parameters required for the calculation of the mutual diffusion coefficients necessary to obtain the diffusional rate coefficients is explained. Next, the experimental polymerization data are presented, and it is shown that controlled piBoA properties are obtained using Cu(I)Br/PMDETA as ATRP catalyst. Then, simulation results are presented illustrating that, as expected from the reports in the literature, βC-scission reactions of mid-chain macroradicals can be neglected in the studied temperature range. Backbiting reactions of end-chain macroradicals are shown to result in a slightly lowering of the polymerization rate and of the level of control of the polymer properties at high conversions. Finally, the effect of diffusional limitations on the ATRP is evaluated based on the population weighted apparent rate coefficients, which are codetermined by the evolution of the apparent rate coefficients as a function of chain length and the chain length distribution (CLD) of the dormant polymer molecules and macroradicals with conversion. A distinction is made between the CLDs related to the end- and mid-chain macromolecular species. It is illustrated that diffusional limitations are significant on termination during the whole polymerization process, whereas on deactivation, diffusional limitations are shown to be important at high conversions only.

4.1. Rheological Measurements: Determination of Hole Free Volume Parameters. The calculation of the mutual diffusion coefficient for a reaction between A and B (D_{AB}; eq 2) depends on the chemical structure of the reactants. For a reaction between non-macromolecules, D_{AB} corresponds to translational (i.e, center-of-mass) diffusion, whereas for reaction steps involving macromolecules, such as deactivation and termination, it can be related to translational and/or segmental diffusion.[16] However, as in ATRP macromolecules with a relatively low chain length are formed, segmental diffusion can be neglected.[15,31,42] Hence, the mutual diffusion coefficient D_{AB} of each reaction can be calculated as the sum of the center-of-mass diffusion coefficients of A and B. For macroradicals, however, also a reaction diffusion coefficient accounting for the motion of the macroradical chain end during a propagation step has to be considered, especially for high mass fractions of polymer (see section 1 of the Supporting Information[29]).[16,43]

The center-of-mass diffusion coefficient of a non-macromolecule A (D_{A}) is calculated as a function of polymerization conditions and conversion based on the Vrentas and Duda free volume theory.[18,19] This theory describes the translational diffusion of a component in the reaction system as a jumping process of (part of) the component into the hole free volume of the reaction system. Diffusion is more difficult for larger molecules or for molecules having more interactions with neighboring molecules. The hole free volume of the reaction system is calculated as the sum of the individual hole free volumes of all pure components. During the ATRP, however, the summed mass fraction of the monomer, the solvent, the internal standard, and the polymer is close to one. Hence, it suffices to calculate the specific hole free volumes of the latter four pure components ($V_{\mathrm{FH},A}$; $A = m, s, is, p$).

In general, the specific hole free volume of a component A, i.e., the available space for A to diffuse per unit of mass, can be calculated via

$$\frac{V_{\mathrm{FH},A}}{\gamma_A} = \frac{K_{1A}}{\gamma_A}\left(K_{2A} - T_{\mathrm{g},A} + T_{\mathrm{pol}}\right) \qquad (3)$$

in which γ_A ($A = m, s, is, p$) is the overlap factor in pure A used to correct for the same hole free volume being available for several jumping units and in which $T_{\mathrm{g},A}$ for the polymer corresponds to its glass transition temperature, while for the

Table 5. Parameters Required for the Calculation of the Specific Hole Free Volume of the Pure Monomer and Solvent, Internal Standard and Polymer ($V_{FH,A}$; $A = m, s, is, p$; eq 3); with for *m*, *s* Also the Related 95% Confidence Intervals and the *F* Value for the Global Significance of the Regression ($F_{tot,calc}$)

A	K_{1A} ($m^3\ kg^{-1}\ K^{-1}$)	$K_{2A} - T_{g,A}$ (K)	$K_{3,A}$ (−)	$F_{tot,calc}$
m[a]	$(1.50 \pm 0.17) \times 10^{-5}$	-245 ± 4	1.42 ± 0.04	3.0×10^{6} [e]
s[a]	$(1.81 \pm 0.03) \times 10^{-7}$	0[b]	(-7.60 ± 0.04)	2.1×10^{6} [e]
is[c]	1.22×10^{-6}	−55.00		
p[d]	3.16×10^{-4}	−271.50		

[a] Via regression of eqs 4 and 5. [b] Not significantly different from zero. [c] From ref 45. [d] Using eqs 6 and 7. [e] Tabulated *F* value for the (global) significance of the regression ($F_{tot,tab}$) = 3.59.

monomer, the internal standard and the solvent it refers to a formally analogous temperature. The parameters K_{1A}/γ_A and $K_{2A} - T_{g,A}$ ($A = m, s, is, p$) in eq 3 can be determined from the measurement of the temperature dependence of the dynamic viscosity of the pure components followed by regression to semiempirical equations. A distinction should be made between the calculation of the specific hole free volume of the non-macromolecules and the macromolecules, as explained in what follows.

4.1.1. Specific Hole Free Volumes of the Non-macromolecules. For the internal standard ($A = is$), K_{1is}/γ_{is} and $K_{2is} - T_{g,is}$ can be taken from literature[45] (see Table 5). For the monomer ($A = m$) and the solvent ($A = s$) K_{1A}/γ_A and $K_{2A} - T_{g,A}$ are obtained from the minimization of the objective function *S* defined by eq 4[44] using a (single response) Levenberg−Marquardt algorithm.[46]

$$S = \sum_{i}^{n_A} (\ln(\eta_A(T_i)) - \ln(\hat{\eta}_A(T_i)))^2 \tag{4}$$

In eq 4, n_A is the number of dynamic viscosity experiments for the component *A* ($A = m, s$) and $\eta_A(T_i)$ and $\hat{\eta}_A(T_i)$ ($i = 1, ..., n_A$) are the measured and the calculated dynamic viscosity of *A* ($A = m, s$) at a temperature T_i. For the calculated dynamic viscosities $\hat{\eta}_A(T_i)$ ($i = 1, ..., n_A$), the Vogel−Fulcher−Tammann−Hesse model[47] is used:

$$\ln(\hat{\eta}_A(T_i)) = K_{3A} + \frac{V_A^*}{\frac{K_{1A}}{\gamma_A}(K_{2A} - T_{g,A} + T_i)} \tag{5}$$

in which K_{3A} is a third parameter to be estimated besides K_{1A}/γ_A and $K_{2A} - T_{g,A}$ ($A = m, s$) and V_A^* is the specific critical hole free volume required for a diffusional jump of *A* (see section 1 of the Supporting Information[29]). To verify the global statistical significance of each regression ($A = m, s$) an *F*-test is used.[48] The statistical significance of the individual parameters is evaluated via the calculation of the 95% individual confidence intervals.

For the solvent, literature data[49] are used for η_s (see section 1 of the Supporting Information[29]). To the best of our knowledge, for the monomer, these data are not available in literature. In this work, η_m was measured via dynamic-mechanical measurements ($\omega = 1\ s^{-1}$) during a temperature ramp with a ramping rate of 0.5 K/min (see section 2.3). The measured dynamic viscosity of the monomer η_m (viz. Figure 2) was found to be well-described using an exponential decay, the parameters of which are given in section 1 of the Supporting Information.[29]

Table 5 presents the estimated parameter values K_{1A}/γ_A, $K_{2A} - T_{g,A}$, and K_{3A} ($A = m, s$), their 95% confidence values, and the *F* value for the global statistical significance of the regression. Both regressions are statistically significant as the *F* values are sufficiently higher than the tabulated ones.

4.1.2. Specific Hole Free Volume of the Macromolecules: WLF Parameters. For the polymer, K_{1p}/γ_p and $K_{2p} - T_{g,p}$ in eq 3 are obtained via[19,45]

$$\frac{K_{1p}}{\gamma_p} = \frac{V_p^*}{2.303 C_1 C_2} \tag{6}$$

$$K_{2p} = C_2 \tag{7}$$

in which C_1 and C_2 are the Williams−Landel−Ferry (WLF) parameters of the polymer piBoA.[50] Note that the latter parameters are related to the Vogel−Fulcher−Tamman−Hesse parameters.[47,51]

In this work, the WLF parameters of piBoA are determined by constructing a master curve from the dynamic moduli measurements followed by regression to

$$S = \sum_{i}^{n_p} (\log(a_T(T_i)) - \log(\hat{a}_T(T_i)))^2 \tag{8}$$

in which n_p is the number of dynamic viscosity experiments for the polymer, T_i is the applied temperature for the *i*th experiment ($i = 1, ..., n_p$), and $a_T(T_i)$ and $\hat{a}_T(T_i)$ are the measured and calculated shift factor at T_i.[51] The shift factors are defined as the ratio of the real and the imaginary part of the modulus (storage and loss modulus $G'(\omega)$ and $G''(\omega)$, respectively) of the polymer at the considered temperature to their counterparts at reference temperature. In this work, the reference temperature T_0 is taken equal to the glass transition temperature of the polymer ($T_{g,p}$), as required for the determination of free volume theory parameters for kinetic modeling studies.[19]

The logarithm of the measured shift factors is presented in Figure 2. The calculated shift factors are obtained from[52]

$$\log(\hat{a}_T(T_i)) = -\frac{C_1(T_i - T_0)}{C_2 + T_i - T_0} \tag{9}$$

Regression to eq 9 leads to a value of 12.1 ± 0.48 and 95.7 ± 5.49 K for C_1 and C_2, respectively. The corresponding equation is also given in Figure 3b. A global significant regression[48] is obtained, as $F_{tot,calc}$ ($= 3.3 \times 10^4$) is much higher than $F_{tot,tab}$ ($= 5.8$). Using eqs 6 and 7, the corresponding values for K_{1p} and $K_{2p} - T_{g,p}$ become 3.16×10^{-4} $m^3\ kg^{-1}\ K^{-1}$ and $-271.50\ K^{-1}$ (see also Table 5), respectively. These WLF parameters have a similar magnitude to those reported by Yamagushi et al.[53] for several other polyacrylates, indicating that the diffusional behavior of piBoA is similar to that of other acrylates.

4.2. Kinetic Study of the ATRP of iBoA. *4.2.1. Experimental Study.* An overview of polymerization conditions investigated in the experimental study is given in Table 1. The experimental data reported pertain to a systematic variation in temperature, initial molar ratio of monomer to initiator, initial molar ratio of activator to initiator, and

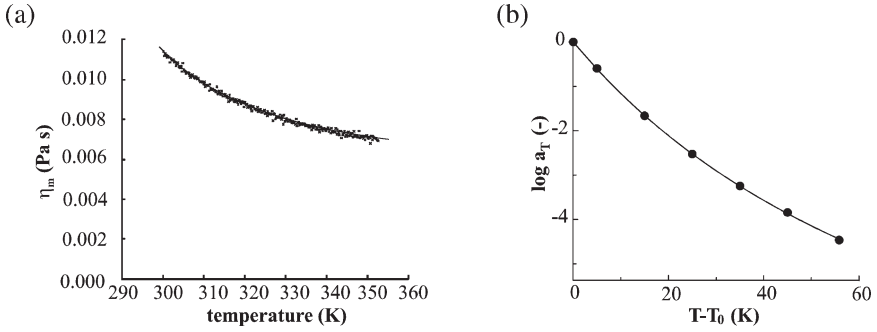

Figure 3. (a) Dynamic viscosity of iBoA (η_m) as a function of temperature; points = experimental data; line = eq 5 (parameters: Table 5 via regression with $F_{tot,calc} = 3.0 \times 10^6$ and $F_{tot,tab} = 3.59$). (b) Shift factor a_T as a function of temperature T for the dynamic viscosity of piBoA (η_p); reference temperature $T_0 = T_{g,p}$; points = measured shift factors; line = eq 9 with $C_1 = 12.1 \pm 0.48$ and $C_2 = 95.7 \pm 5.49$ K obtained from regression to the measured shift factors with $F_{tot,calc} = 3.3 \times 10^4$ and $F_{tot,tab} = 5.8$.

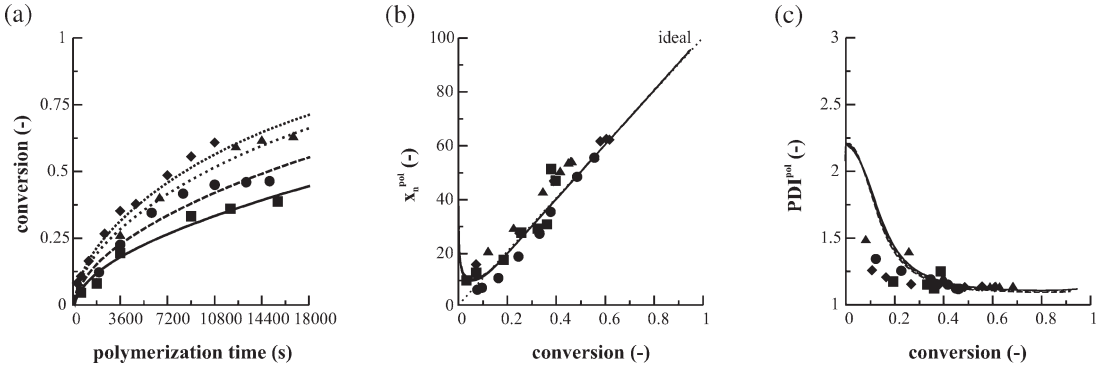

Figure 4. Effect of the temperature (T_{pol}) on (a) the conversion (x_m) profile, (b) the average chain length of the polymer molecules (x_n^{pol}), and (c) the polydispersity index of the MMD of the polymer (PDI^{pol}). Conditions: [*i*BoA]$_0$/[MBP]$_0$/[Cu(I)Br]$_0$/[PMDETA]$_0$ = 100/1/1.5/1.5, [Cu(II)Br$_2$]$_0$ = 0 mol m^{-3} and 33.3 vol % ethyl acetate with respect to iBoA; experimental points/simulated (kinetic parameters: Table 2): (■/—) T_{pol} = 323 K, (●/– –) T_{pol} = 333 K, (▲/--) T_{pol} = 343 K, and (◆/···) T_{pol} = 348 K (i.e., entries 1, 2, 5, and 8 in Table 1); ideal $x_n^{pol} = [M]_0/[R_0X]_0 x_m$ (dashed linear line).

initial molar ratio of deactivator to initiator. For each studied polymerization condition, the conversion (x_m) and the level of control of the ATRP with respect to chain length are tracked during the ATRP. The ATRP process is labeled as highly controlled if the average chain length is close to the ideal one, i.e., almost equal to $x_n^{pol} = [M]_0/[R_0X]_0 x_m$[54] and the polydispersity index (PDI^{pol}) is below ca. 1.4 as a function of conversion, both from sufficiently high conversions onward.

In Figure 4a–c the effect of temperature (T_{pol}) on the conversion profile and the level of control of the ATRP with respect to chain length is shown for an initial molar ratio of monomer to initiator equal to 100. Note that the maximum temperature is determined by the boiling point of the solvent (i.e., 350 K[55]). On the basis of the extrapolation of the measured conversion profile, it can be inferred that, at 323 K, it would take about 20 h to reach a conversion of 0.8 (see Figure 4), whereas at 348 K only 7 h is required. Figure 4b,c illustrates that the effect of an increase in temperature on the level of control with respect to chain length on the ATRP is negligible. At all temperatures studied, highly controlled ATRPs are obtained; from a conversion of ca. 0.15 on, the average chain lengths almost coincide with the ideal ones and the polydispersity indices remain below 1.4. Note that, at higher temperatures, a limiting value around 1.15 (i.e., a value close to 1) is observed for the polydispersity index at high conversions. It can hence be concluded that the use of higher temperatures seems more appropiate, as a fast ATRP is obtained with a high level of control.

As illustrated in Figure 5c, the PDI^{pol} profile is only slightly affected by the initial molar ratio of deactivator to initiator. It should be noted that the experimental data in case deactivator is initially present are limited to low conversions at which a higher experimental error on the measured PDI^{pol} can be expected. The initial presence of deactivator results in slightly lower PDI^{pol} values but is offset by a much slower polymerization (viz. Figure 5a). Clearly, the improvement of the level of control with respect to chain length by the initial presence of deactivator is limited (viz. Figure 5b,c) as, in the absence of deactivator, the PDI^{pol} values are already rather close to one and the related x_n^{pol} profile almost coincides with the ideal one. Hence, the use of nonzero initial deactivator concentrations should be avoided.

Figure 6a shows that, as expected, the polymerization rate is higher for a lower initial molar ratio of monomer to initiator ([iBoA]$_0$/[MBP]$_0$; T_{pol} = 343 K). The PDI^{pol} profile, on the other hand, remains practically unchanged by the initial molar ratio of monomer to initiator.

Figure 7a–c presents the conversion, x_n^{pol}, and PDI^{pol} profile for various initial molar ratios of activator and initiator. Clearly, at a given temperature, the polymerization rate increases with increasing initial molar ratio of activator to initiator. The level of the control of the ATRP with respect to chain length (Figure 7b,c) is, however, similar for all studied conditions. Hence, a high level of control with respect to chain length can be obtained for piBoA using a reduced ATRP catalyst concentration.

4.2.2. Importance of Backbiting and βC-Scission Reactions. In Figures 4a–7c the obtained simulation results using the Arrhenius and thermodynamic parameters in Table 2 are presented for the experimentally investigated polymerization conditions in Table 1. It can be seen that the experimental trends of the conversion, average chain length, and polydispersity index profiles are captured by the kinetic model reasonably well. The kinetic model also allows simulating the

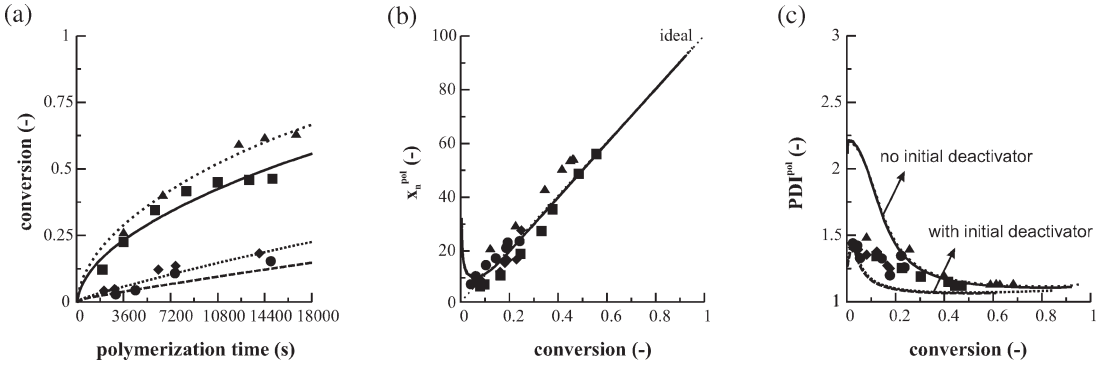

Figure 5. Effect of the initial presence of deactivator on (a) the conversion (x_m) profile, (b) the average chain length of the polymer molecules (x_n^{pol}), and (c) the polydispersity index of the MMD of the polymer (PDI^{pol}). Conditions: $[iBoA]_0/[MBP]_0/[Cu(I)Br + Cu(II)Br_2]_0/[PMDETA]_0$ = 100/1/1.5/1.5 and 33.3 vol % ethyl acetate with respect to iBoA; experimental points/simulated (kinetic parameters: Table 2): (■/—) T_{pol} = 333 K and $[Cu(II)Br_2]_0/([Cu(I)Br + Cu(II)Br_2]_0)$ = 0, (●/−−) T_{pol} = 333 K and $[Cu(II)Br_2]_0/([Cu(I)Br + Cu(II)Br_2]_0)$ = 0.05, (▲/--) T_{pol} = 343 K and $[Cu(II)Br_2]_0/([Cu(I)Br + Cu(II)Br_2]_0)$ = 0, and (◆/···) T_{pol} = 343 K and $[Cu(II)Br_2]_0/([Cu(I)Br + Cu(II)Br_2]_0)$ = 0.05 (i.e., entries 2, 3, 5, and 6 in Table 1); ideal $x_n^{pol} = [M]_0/[R_0X]_0 x_m$ (dashed linear line).

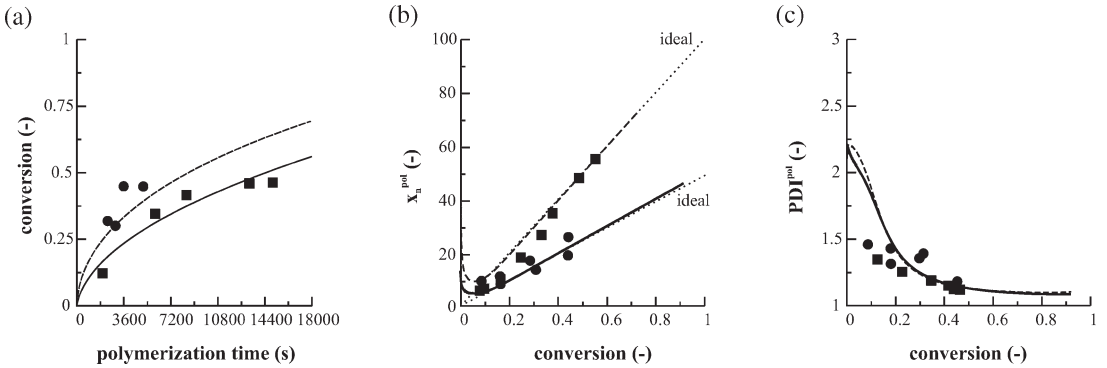

Figure 6. Effect of the initial molar ratio of the monomer to the initiator ($[iBoA]_0/[MBP]_0$) on (a) the conversion (x_m) profile, (b) the average chain length of the polymer molecules (x_n^{pol}), and (c) the polydispersity index of the MMD of the polymer (PDI^{pol}). Conditions: $[MBP]_0/[Cu(I)Br]_0/[PMDETA]_0$ = 1/1.5/1.5, $[Cu(II)Br_2]_0$ = 0 mol m^{-3}, T_{pol} = 333 K and 33.3 vol % ethyl acetate with respect to iBoA; experimental points/simulated (kinetic parameters: Table 2): (■/—) $[iBoA]_0/[MBP]_0$ = 100, (●/−−) $[iBoA]_0/[MBP]_0$ = 50 (i.e., entries 2 and 4 in Table 1); ideal $x_n^{pol} = [M]_0/[R_0X]_0 x_m$ (dashed linear line).

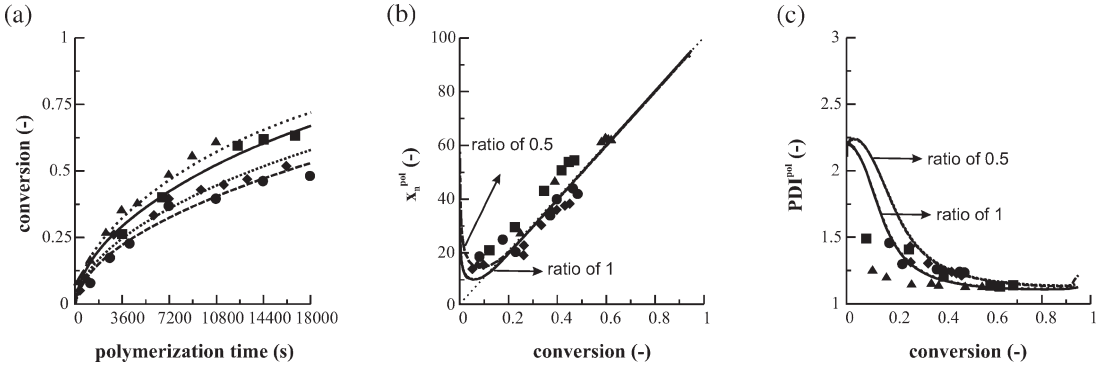

Figure 7. Effect of the initial molar ratio of copper(I) bromide to the initiator ($[Cu(I)Br]_0/[MBP]_0$) on (a) the conversion (x_m) profile, (b) the average chain length of the polymer molecules (x_n^{pol}), and (c) the polydispersity index of the MMD of the polymer (PDI^{pol}). Conditions: $[iBoA]_0/[PMDETA]_0$ = 100/1.5, $[Cu(II)Br_2]_0$ = 0 mol m^{-3} and 33.3 volume percentage ethyl acetate with respect to iBoA; experimental points/simulated (kinetic parameters: Table 2): (■/—) T_{pol} = 343 K and $[Cu(I)Br]_0/[MBP]_0$ = 1, (●/−−) T_{pol} = 343 K and $[Cu(I)Br]_0/[MBP]_0$ = 0.5, (▲/--) T_{pol} = 348 K and $[Cu(I)Br]_0/[MBP]_0$ = 1, and (◆/···) T_{pol} = 348 K and $[Cu(I)Br]_0/[MBP]_0$ = 0.5 (i.e., entries 5, 7, 8, and 9 in Table 1); ideal $x_n^{pol} = [M]_0/[R_0X]_0 x_m$ (dashed linear line).

end-group functionality and the short-chain branching and CC double-bond content as a function of conversion. For the calculation of the latter polymer properties, the reader is referred to section 5 of the Supporting Information. Both contents are expressed as a mol % per average number of monomer units. In what follows, simulation results of the end-group functionality and the short-chain branching and CC double-bond content as a function of conversion are discussed for the lowest and highest temperature investigated (i.e., 323 and 348 K; polymerization conditions 1 and 8 in Table 1).

From Figure 8a it follows that only a limited loss of polymer end-group functionality occurs during the ATRP, as polymer end-group functionalities above 0.98 are obtained. Hence, besides a high level of control of chain length, highly living polymers result for the ATRP of iBoA.

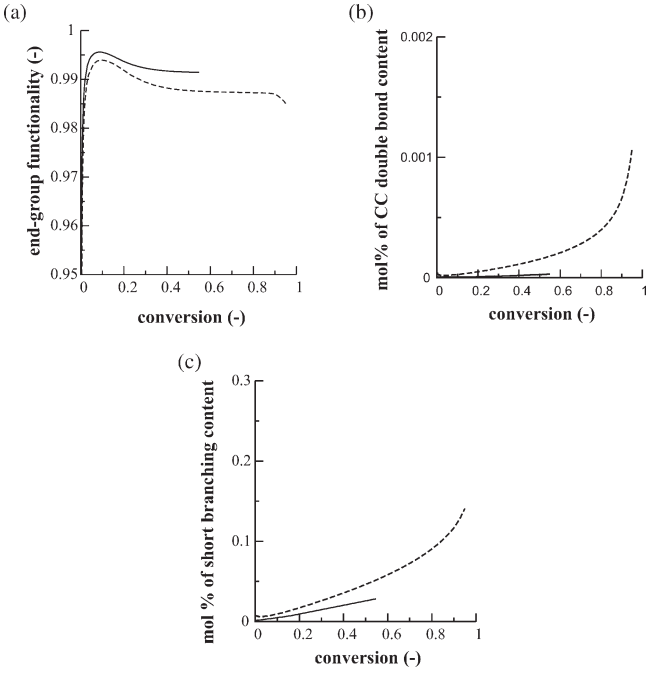

Figure 8. (a) End-group functionality, (b) the mol % of CC double-bond content (expressed per average number of monomer units) as a function of conversion, and (c) the mol % of short-chain branching (expressed per average number of monomer units) as a function of conversion for entry 1 (323 K; full line) and entry 8 (348 K; dashed line) in Table 1. Kinetic parameters: Table 2.

At 348 K, however, it can be seen that the loss of end-group functionality becomes slightly more pronounced. At higher temperatures, activation is more favored, and at low conversions higher radical concentrations are obtained, leading to an increased importance of termination reactions and consequental loss of end-group functionality.

Figure 8b presents the simulated CC double-bond content as a function of conversion for both temperatures. The simulated CC double-bond content is found to be extremely low (< 0.0015 mol %), confirming that βC-scission reactions in the ATRP of iBoA can be neglected at temperatures up to 350 K. This outcome is in agreement with the absence of unsaturations in the ^{13}C NMR spectra reported by Ahmad et al.[7] for the ATRP of *n*-BuA using the same ATRP catalyst. However, it should be noted that the relative importance of βC-scission reactions increases with increasing conversions, i.e., at lower monomer concentrations, and with increasing temperature. This is in agreement with literature data for *n*-BuA; at 411 K under starved-feed conditions only, the importance of βC-scission reactions has shown to be high.[5]

In Figure 8c the simulated short branching content is given as a function of conversion for both temperatures. For the ATRP of *n*-BuA using the same ATRP catalyst, Ahmad et al.[7] recently measured a branching content of 0.40−0.70 mol % at 353 K at almost complete conversion. These authors also indicated that similar branching contents can be expected for the ATRP of other acrylates. From the data presented by Ahmad et al.,[7] it can be expected that, for iBoA, the branching content remains below 0.50 mol % at 348 K, the highest temperature investigated in this work, as backbiting is strongly activated and iBoA end-chain macroradicals are very likely to be less prone to backbiting reactions than *n*-BuA end-chain macroradicals. From Figure 8c, it can be seen that a branching content around 0.2 mol % is obtained at 348 K at almost complete conversion, in agreement with expectations. Note that at 323 K a less pronounced increase of the branching content with conversion can be observed.

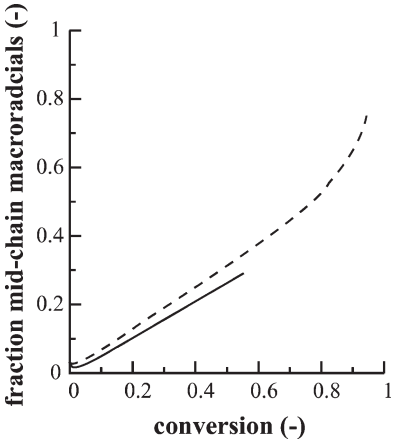

Figure 9. Fraction of mid-chain macroradicals as a function of conversion for entry 1 (323 K; full line) and entry 8 (348 K; dashed line) in Table 1. Kinetic parameters: Table 2.

The increased importance of backbiting reactions at higher conversions can also be clearly seen in Figure 9 in which the fraction of mid-chain macroradicals is presented as a function of conversion for both temperatures. At 348 K, at conversions higher than 0.8, the fraction of mid-chain macroradicals becomes the dominant fraction, whereas at 323 K this would be expected at a conversion of 0.9, based on extrapolation of the simulation results. Note that the application of the quasi-steady state approximation to the mid-chain macroradicals, as in often done in the literature, is cleary unvalid in this case. The obtained concentration profile of the mid-chain macroradicals indicates that the production and consumption rate of these radicals are clearly different at low and high conversions.

To evaluate the influence of backbiting reactions, simulations were also performed in which backbiting reactions were removed from the kinetic model and compared with simulations obtained using the full kinetic model (viz. Figure 10a−d). It can be seen in Figure 10a that the decrease of the polymerization rate due to backbiting reactions remains limited at 323 K while it becomes more pronounced at 348 K, in particular at higher conversions. No influence of backbiting reactions on the simulated average chain length profile is, however, observed (viz. Figure 10b). The influence of backbiting reactions on the simulated PDI^{pol} and end-group functionality profiles (viz. Figure 10c,d) is limited.

The decrease of the polymerization rate due to backbiting reactions can be explained by the significantly lower intrinsic chemical rate coefficient for propagation of mid-chain macroradicals compared to end-chain macroradicals. The differences between the simulated PDI^{pol} and end-group functionality profiles by both kinetic models suggest a limited disturbance of the normal activation−growth−deactivation process each time backbiting occurs.

Hence, it can be concluded based on the PLP study of Dervaux et al.[8] and the simulation results obtained in this work that the effect of backbiting reactions on the ATRP of iBoA in the temperature range 325−348 K is limited. A relatively low branching content (around 0.2 mol %) is obtained at higher conversions and temperatures (> 348 K). From low to intermediate conversions and at lower temperatures (< 323 K) backbiting reactions are of minor importance and, hence, have only a limited influence on the polymerization rate and the polymer properties.

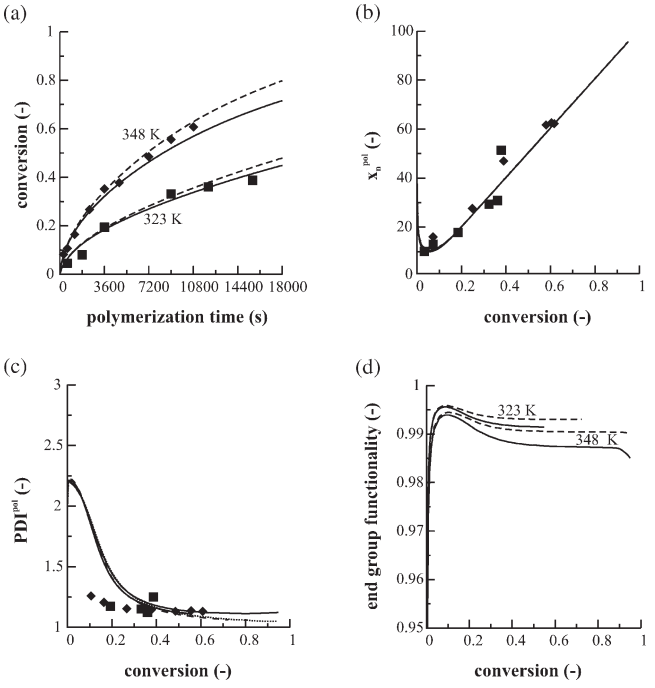

Figure 10. (a) Conversion profile, (b) the average chain length of the polymer molecules (x_n^{pol}), (c) the polydispersity index of the MMD of the polymer (PDI^{pol}), and (d) the fraction of polymer molecules having end-group functionality (f_p) as a function of conversion (x_m) for entry 1 (323 K) and entry 8 (348 K) in Table 1; full lines with backbiting; dashed lines without backbiting; kinetic parameters: Table 2; experimental points: (■) T_{pol} = 323 K and (◆) T_{pol} = 348 K.

Table 6. Values of the Center-of-Mass Diffusion Coefficient of a Non-macromolecule A (D_A) at T_{pol} = 335 K, $w_m = w_s = w_p$ = 0.33, and w_{is} = 0.01

A	name	D_A (m^2 s^{-1})
1	iBoA	2.32×10^{-10}
2	MBP	3.49×10^{-8}
3	M(.)P [a]	1.84×10^{-8}
4	[Cu(I)BrPMDETA] [b]	1.06×10^{-8}
5	[Cu(II)Br$_2$PMDETA] [b]	4.60×10^{-9}
6	ethyl acetate	1.98×10^{-8}
7	*n*-decane	5.08×10^{-9}

[a] Initiating radical from MBP. [b] From ref 17 with $D_{0,A}^{av}$ (see section 4 of the Supporting Information[29]) evaluated at T_{pol} = 335 K.

4.2.3. Importance of Diffusional Limitations

Apparent Rate Coefficients. As indicated above, diffusional limitations on a reaction step are accounted for by the calculation of an apparent rate coefficient consisting of a diffusional and an intrinsic chemical rate coefficient. It should however be noted that for reactions steps that are characterized by a relatively high intrinsic chemical rate coefficient, such as termination ($k_{tc,chem} \approx 10^6$ m^3 mol^{-1} s^{-1}) and deactivation ($k_{da,chem} \approx 10^5$ m^3 mol^{-1} s^{-1}), diffusional limitations are more likely to occur than reactions with a relatively low intrinsic chemical rate coefficient, such as propagation ($k_{p,chem} \approx 10$ m^3 mol^{-1} s^{-1}) and activation ($k_{a,chem} \approx 10^{-4}$ m^3 mol^{-1} s^{-1}).

Table 6 presents the obtained values of the center-of-mass diffusion coefficients of the non-macromolecules using the Vrentas and Duda free volume theory for a mass fraction of monomer, solvent, and polymer of 0.33 and a mass fraction of 0.01 for the internal standard at 335 K (i.e., at the average temperature of the investigated temperature range). It can be seen that the center-of-mass diffusion coefficient for the monomer iBoA is significantly lower than for the other non-macromolecules, consistent with the relatively high value measured for the dynamic viscosity of iBoA. Hence, an important effect of diffusional limitations during the ATRP of iBoA can be expected.

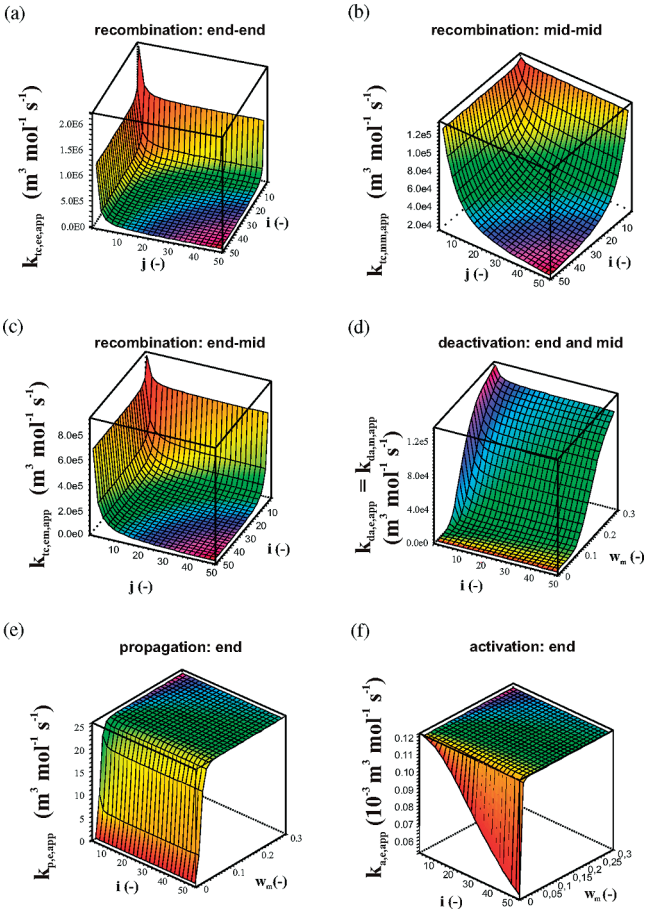

Figure 11. Apparent rate coefficient for termination by recombination beween (a) end-chain macroradicals ($k_{tc,ee,app}$), (b) mid-chain macroradicals ($k_{tc,mm,app}$), and (c) their cross-termination ($k_{tc,em,app}$) as a function of the chain length of the macroradicals (*i*, *j*) at 335 K for a monomer and solvent mass fraction of 0.30 and a mass fraction of internal standard equal to 0.05. (d) Apparent rate coefficient for deactivation with end- and mid-chain macroradicals ($k_{da,e,app}$ and $k_{da,m,app}$; equal intrinsic chemical rate coefficients) and (e) for propagation with end-chain macroradicals ($k_{p,e,app}$) as a function of the chain length of the macroradicals *i* and the monomer mass fraction. (f) Apparent rate coefficient for activation ($k_{a,e,app}$) with end-chain dormant polymer molecules as a function of the chain length of the dormant polymer molecule (*i*) and the monomer mass fraction (w_m) at 335 K for a solvent mass fraction of 0.30 and a mass fraction of internal standard equal to 0.05; activation rescaled (multiplied by 10^3). Kinetic parameters: Table 2.

Figure 11a−c presents the apparent rate coefficients for termination by recombination between end-chain macroradicals and mid-chain macroradicals and for cross-recombination ($k_{tc,ee,app}$, $k_{tc,em,app}$, and $k_{tc,mm,app}$) as function of chain length at 335 K for a monomer and solvent mass fraction of 0.30 and a mass fraction of internal standard equal to 0.05. A significant decrease of $k_{tc,ee,app}$ can be observed for higher chain lengths. For recombinations involving mid-chain macroradicals, a similar although slightly less pronounced effect is observed, as they are characterized by a lower intrinsic chemical rate coefficient compared to recombinations involving end-chain macroradicals (Table 2). Note that the observed decrease of these apparent rate coefficients is predominantly determined by the decrease of the center-of-mass contribution to the corresponding diffusional rate coefficients (see section 1 of the Supporting Information[29]).

As can be seen in Figure 11d, also the apparent rate coefficients for deactivation of end-chain and mid-chain radicals ($k_{da,e,\mathrm{app}}$ and $k_{da,m,\mathrm{app}}$) decrease for high chain lengths, however, only at high conversions. Note that no difference is observed between deactivation of end- and mid-chain macroradicals as both are assumed to be characterized by the same intrinsic chemical rate coefficient (Table 2). For deactivation, the diffusional rate coefficient is mainly determined by the center-of-mass diffusion coefficient of the deactivator, a non-macromolecule, resulting in a high importance of diffusional limitations at high conversions only (see section 1 of the Supporting Information[29]).

In contrast, for propagation and activation of end-chain and mid-chain macromolecular species, it follows from Figure 11e,f (end-chain macromolecular species) and Figure 2a,b in section 1 of the Supporting Information[29] (mid-chain macromolecular species) that only at extremely high conversions (close to complete conversion) a significant decrease of the corresponding apparent rate coefficients $k_{p,e,\mathrm{app}}$ and $k_{a,e,\mathrm{app}}$, $k_{p,m,\mathrm{app}}$ and $k_{a,m,\mathrm{app}}$ is obtained. Propagation and activation are therefore reaction controlled as diffusion of the related reaction components occurs fast enough.

It can be concluded that only the termination and deactivation rates of end- and mid-chain macromolecular species will strongly be influenced by molecular diffusion phenomena, especially once the contribution of the higher chain lengths to the radical population becomes important. In what follows, the combined effect of the apparent rate coefficients and the related CLDs is discussed.

Population-Weighted Apparent Rate Coefficients. Figure 12 presents the evolution of the population-weighted apparent rate coefficients (zeroth order) for termination by recombination between end-chain macroradicals ($\langle k_{tc,ee,\mathrm{app}},0\rangle$) and mid-chain macroradicals ($\langle k_{tc,mm,\mathrm{app}},0\rangle$) and their cross-termination ($\langle k_{tc,em,\mathrm{app}},0\rangle$) and for deactivation of end-chain macroradicals ($\langle k_{da,e,\mathrm{app}},0\rangle$) and of mid-chain macroradicals ($\langle k_{da,m,\mathrm{app}},0\rangle$) as defined by eqs 10−12 for a representative polymerization condition (entry 8 in Table 1).

$$\langle k_{tc,ee/mm,\mathrm{app}},0\rangle = \frac{\sum_{i=1/3}^{\infty}\sum_{j=1/3}^{\infty} k^{ij}_{tc,ee/mm,\mathrm{app}} R_{i,e/m} R_{j,e/m}}{\left[\sum_{i=1/3}^{\infty} R_{i,e/m}\right]^2} \tag{10}$$

$$\langle k_{tc,em,\mathrm{app}},0\rangle = \frac{\sum_{i=1}^{\infty}\sum_{j=3}^{\infty} k^{ij}_{tc,em,\mathrm{app}} R_{i,e} R_{j,m}}{\left[\sum_{i=1}^{\infty} R_{i,e}\right]\left[\sum_{j=3}^{\infty} R_{j,m}\right]} \tag{11}$$

$$\langle k_{da,e/m,\mathrm{app}},0\rangle = \frac{\sum_{i=1/3}^{\infty} k^{i}_{da,e/m,\mathrm{app}} R_{i,e/m}}{\sum_{i=1/3}^{\infty} R_{i,e/m}} \tag{12}$$

In eqs 10−12, $k^{ij}_{tc,ee,\mathrm{app}}$, $k^{ij}_{tc,mm,\mathrm{app}}$, and $k^{ij}_{tc,em,\mathrm{app}}$ are the apparent rate coefficient for termination by recombination between end-chain macroradicals having a chain length i and j, between mid-chain macroradicals having a chain length i and j, and between an end-chain macroradical having a chain length i and a mid-chain macroradical having a chain length j. Furthermore, $k^{i}_{da,e,\mathrm{app}}$ and $k^{i}_{da,m,\mathrm{app}}$ are the apparent rate coefficient for deactivation of an end-chain and mid-chain macroradical having a chain length i and $R_{i,e}$ and $R_{i,m}$ are the concentration of end-chain and mid-chain macroradicals having a chain length i. In section 6 of the Supporting Information the analogous figures for propagation of end- and mid-chain macroradicals and for activation of end- and mid-chain dormant polymer molecules are given.

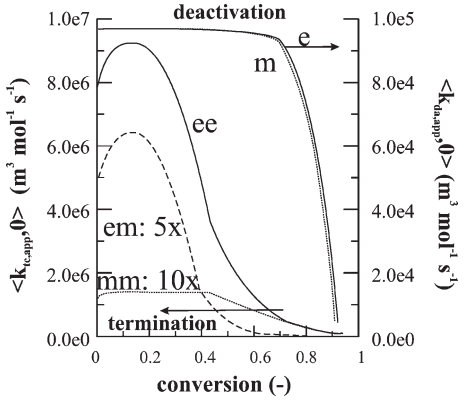

Figure 12. Population-weighted (zeroth-order) apparent rate coefficient for termination (by recombination) between end-chain macroradicals (full line; left y-axis; $\langle k_{tc,ee,\mathrm{app}},0\rangle$), between mid-chain macroradicals (dotted line; left y-axis; mulitplied by 10; $\langle k_{tc,mm,\mathrm{app}},0\rangle$) and for the corresponding cross-termination ($\langle k_{tc,em,\mathrm{app}},0\rangle$; dashed line; multiplied by 5; left y-axis) and for deactivation with end- and mid-chain macroradicals (full and dotted line; right y-axis; $\langle k_{da,e,\mathrm{app}},0\rangle$ and $\langle k_{da,m,\mathrm{app}},0\rangle$) as a function of conversion for entry 8 in Table 1. Kinetic parameters: Table 2; eqs 10−12.

It can be seen in Figure 12 that during the ATRP the population-weighted apparent rate coefficients for termination change significantly. After a weak increase at low conversion they strongly decrease at higher conversions, indicating an important influence of diffusional limitations on termination during the ATRP. Note that in agreement with the apparent rate coefficients the effect of diffusional limitations changes from very pronounced to pronounced for $\langle k_{tc,ee,\mathrm{app}},0\rangle$, $\langle k_{tc,em,\mathrm{app}},0\rangle$, and $\langle k_{tc,mm,\mathrm{app}},0\rangle$. However, it should be kept in mind that at low to intermediate conversions the contribution of mid-chain macroradicals is low (viz. Figure 9), and hence, at these conversions termination reactions occur predominantly between end-chain macroradicals.

The initial increase of $\langle k_{tc,ee,\mathrm{app}},0\rangle$, $\langle k_{tc,mm,\mathrm{app}},0\rangle$, and $\langle k_{tc,em,\mathrm{app}},0\rangle$ can be related to the movement of the CLDs of the end-chain and mid-chain macroradicals and the corresponding dormant polymer molecules with conversion. In Figure 13a−d the movement of the mass CLDs, i.e., the mass fraction of the macromolecules as a function of their chain length, is presented. For a detailed description of the calculation of these CLDs the reader is referred to ref 17 and section 4 of the Supporting Information.

It can be seen in Figure 13a−c that the mass CLDs of the macroradicals and dormant polymer molecules are almost identical. The latter reflects the high importance of the activation−deactivation process during the ATRP. Furthermore, as end- and mid-chain macroradicals are interconverted by backbiting and subsequent propagation, minor differences between the CLDs of end-chain and mid-chain macromolecular species can be expected. These figures also indicate that, initially, higher chain lengths contribute significantly to the CLDs leading to tail formation. At very low conversions, deactivation is relatively less important; i.e., the so-called persistent radical effect[56] is not fully operative yet, and initiating radicals can add several monomer units before they become deactivated explaining the relatively high initial contribution of high chain lengths to the CLDs. Until conversions up to 0.2, deactivation gradually gains in importance

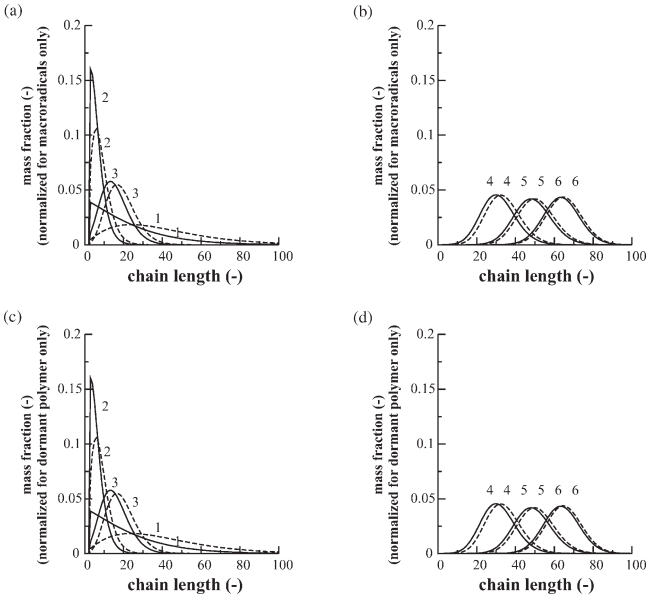

Figure 13. Mass chain length distribution (CLD) of the end- and mid-chain macroradicals (a) + (b) and of the dormant polymer molecules (c) + (d) as a function of conversion (x_m). Kinetic parameters: Table 2; 1: $x_m = 0.005$; 2: $x_m = 0.20$; 3: $x_m = 0.30$; 4: $x_m = 0.50$; 5: $x_m = 0.60$; 6: $x_m = 0.70$; for entry 8 in Table 1; full lines: end-chain macroradicals; dotted lines: mid-chain macroradicals.

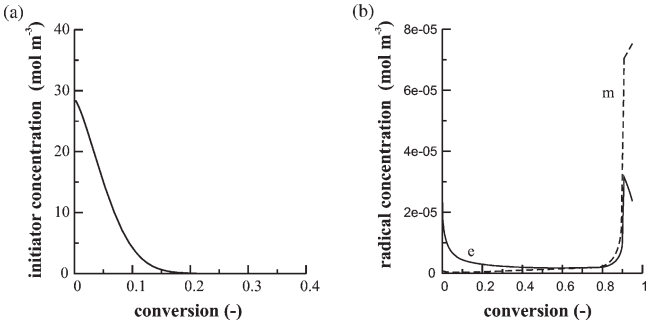

Figure 14. (a) Initiator and (b) end-/mid-chain macroradical concentration (*e*/*m*) as a function of conversion for entry 8 in Table 1. Kinetic parameters: Table 2.

and newly initiated radicals are deactivated after less propagaton steps, leading to an increased contribution of lower chain lengths to the CLDs. As the apparent termination rate coefficient is higher for macroradicals with lower chain lengths, the increased contribution of the lower chain lengths to the CLDs explains the initial increase of $\langle k_{tc,ee,\mathrm{app}},0\rangle$, $\langle k_{tc,mm,\mathrm{app}},0\rangle$, and $\langle k_{tc,em,\mathrm{app}},0\rangle$ in Figure 12.

Once initiation is completed (i.e., at $x_m > 0.2$; viz. Figure 14a), the chain length of the dormant species is gradually increased in each activation−growth−deactivation cycle resulting in a gradual shift of the CLDs to higher conversions (viz. Figure 13a−d). Hence, at conversions at which backbiting becomes important (viz. Figure 10a−d and Figure 9), the fraction of "short-chain radicals" is low and the assumption of a chain length independent rate coefficient for backbiting is justified. Moreover, the increased contribution of the higher chain lengths at higher conversions leads to a decrease of $\langle k_{tc,ee,\mathrm{app}},0\rangle$, $\langle k_{tc,em,\mathrm{app}},0\rangle$, and $\langle k_{tc,mm,\mathrm{app}},0\rangle$. As the diffusional rate coefficient for macroradicals having a higher chain length fastly decrease with increasing conversion, $\langle k_{tc,ee,\mathrm{app}},0\rangle$, $\langle k_{tc,em,\mathrm{app}},0\rangle$, and $\langle k_{tc,mm,\mathrm{app}},0\rangle$ decrease strongly at higher conversions.

In contrast, for deactivation, the decrease of the population-weighted apparent rate coefficients $\langle k_{da,e,\mathrm{app}},0\rangle$ and $\langle k_{da,m,\mathrm{app}},0\rangle$ is limited to high conversions only as illustrated in Figure 12, in agreement with the behavior of the apparent rate coefficients as discussed above. It should be noted that this decrease of $\langle k_{da,e,\mathrm{app}},0\rangle$ and $\langle k_{da,m,\mathrm{app}},0\rangle$ results in an increase of the end-chain and mid-chain macroradical concentration at conversions above 0.9 (viz. Figure 14b) and, hence, in an increased occurrence of termination reactions at high conversions. Indeed, in Figure 10d it can be seen that at high conversions the polymer end-group functionality is characterized by a drop at conversions above 0.9.

Finally, for propagation and activation, the corresponding population weighted apparent rate coefficients $\langle k_{p,e,\mathrm{app}},0\rangle$ and $\langle k_{a,e,\mathrm{app}},0\rangle$, $\langle k_{p,m,\mathrm{app}},0\rangle$, and $\langle k_{a,m,\mathrm{app}},0\rangle$ (see section 6 of the Supporting Information) remain constant up to very high conversions as was already inferred from the above discussion of the behavior of the apparent rate coefficients.

5. Conclusions

Dynamic viscosities of iBoA at temperatures ranging from 280 to 350 K and of piBoA at temperature higher than $T_{g,p}$ and the related WLF parameters are reported. For the ATRP of iBoA in ethyl acetate with MBP as initiator, copper bromide as transition metal salt, and PMDETA as ligand these data are used to calculate the hole free volume as a function of conversion and hence the corresponding apparent rate coefficients.

In the investigated temperature range (323−348 K) for the ATRP of iBoA the occurrence of βC-scission reactions is insignificant, and the importance of backbiting reactions is limited to high conversions. Only from a conversion of ca. 0.8−0.9 onward the fraction of mid-chain macroradicals becomes clearly dominant, and backbiting reactions result in a slight decrease of the polymerization rate and of the level of control and this more pronounced at higher temperatures. Both decreases can be mainly attributed to the slower propagation of mid-chain macroradicals compared to end-chain macroradicals disturbing the regular activation−growth−deactivation process. The effect of backbiting reactions on the polymer end-group functionality and the average chain length of the polymer molecules is limited.

The importance of diffusional limitations is more pronounced on termination than on deactivation. At low conversions an increase of the population-weighted apparent rate coefficients for termination reactions with end- and mid-chain macroradicals is obtained as the CLDs of the end- and mid-chain macroradicals shift to lower chain lengths. At higher conversions, the CLDs shift gradually to higher chain lengths for which diffusional limitations become stronger leading to a reduced importance of termination reactions. The decrease of the population-weighted apparent for deactivation due to diffusional limitations is limited to high conversions only and can result in a decrease of the polymer end-group functionality.

Acknowledgment. The Institute for the Promotion of Innovation through Science and Technology in Flanders (IWT Vlaanderen), the Belgian Government (IAP/IUAP/PAI P6/27: "Functional Supramolecular Systems"), 'la Communauté Française de Belgique' and the Research Foundation-Flanders (FWO) are acknowledged for financial support.

Supporting Information Available: Calculational details concerning: (i) the diffusional and (population weighted) apparent rate coefficients; (ii) the regression analysis for the determination of the Arrhenius and thermodynamic parameters for reactions involving secondary end-chain macroradicals; (iii) the volume of the reaction mixture; (iv) the dynamic viscosity of the monomer and solvent; (v) the extension of the kinetic modeling for

ATRP to reactions involving tertiary mid-chain macroradicals; and (vi) the short chain and CC double bond content. This material is available free of charge via the Internet at http://pubs.acs.org.

Notation

a = root-mean-square end-to-end distance per square root of the number of monomer units in a polymer molecule [m]
a_T = shift factor for dynamic viscosity of the polymer [−]
A_a = pre-exponential factor for activation [m^3 mol^{-1} s^{-1}]
A_t = pre-exponential factor for termination [m^3 mol^{-1} s^{-1}]
[C] = concentration of C [mol m^{-3}]
C_1 = first WLF parameter [−]
C_2 = second WLF parameter [K]
D_A = self-diffusion coefficient of the (reaction) component A [m^2 s^{-1}]
D_{AB} = mutual diffusion coefficient for reaction between molecules A and B [m^2 s^{-1}]
$D_{0,A}^{av}$ = average pre-exponential factor for the center-of-mass diffusion coefficient of the reaction component A [m^2 s^{-1}]
E_A = activation energy [(k)J mol^{-1}]
E_{coh} = cohesive energy [(k)J mol^{-1}]
F = F value [−]
G' = storage modulus [Pa]
G'' = loss modulus [Pa]
Hg = mercury (unit for atmosperic pressure)
is_0 = initial mass of the internal standard [kg]
K = first Mark−Houwink constant for a polymer−solvent system [dL g^{-1}]
K_{eq} = ATRP equilibrium coefficient of the activation deactivation process [−]
K_{1A} = parameter for specific hole free volume of pure reaction component A [m^3 kg^{-1} K^{-1}]
$K_{2A} - T_{g,A}$ = parameter for specific hole free volume of pure reaction component A [K]
K_{3A} = parameter in the Vogel−Fulcher−Tammann−Hesse model [−]
k = rate coefficient [m^3 mol^{-1} s^{-1}]
L = ligand [−]
l = reaction step [−]
M = monomer (concentration) [(mol m^{-3})]
M_q = macromonomer (concentration) (chain length q) [(mol m^{-3})]
MM_A = molar mass of the (reaction) component A [kg mol^{-1}]
$MM_{j,B}$ = molar mass of the jumping unit of the (reaction) component B [kg mol^{-1}]
$M_t^n L_y X$ = activator (concentration) [(mol m^{-3})]
$M_t^{n+1} L_y X_2$ = deactivator (concentration) [(mol m^{-3})]
m = number of responses [−]
m_0 = initial mass of the monomer [kg]
M_n = number-average molar mass of the polymer [kg mol^{-1}]
n = number of samples (related to the polymerization experiments) [−]
n_A = number of dynamic viscosity experiments for the (reaction) component A [−]
N_A = Avogrado constant [mol^{-1}]
par = parameter in the correlation for η_m [−]
P_i = dead polymer molecule with chain length i ($i > 0$) [−]
PDI^{pol} = polydispersity index of the MMD of the polymer [−]
R = universal gas constant [J mol^{-1} K^{-1}]
$\langle R^2 \rangle$ = mean-square end-to-end distance [m^2]
R_i = macroradical with chain length i ($i > 0$) [−]
R_{ini} = initiating radical (or R_i with $i = 0$) [−]
$R_{ini}X$ = initiator (or $R_i X$ with $i = 0$) [−]
$R_i X$ = dormant polymer molecule with chain length i ($i > 0$) [−]
R_0 = initiating radical (or R_{ini}) [−]
$R_0 X$ = initiator (or $R_{ini}X$) [−]
s_0 = initial mass of the solvent [kg]
S = merit function [−]
T = temperature [K]
T_0 = reference temperature for WLF parameters [K]
T_{pol} = (polymerization) temperature [K]
$T_{g,p}$ = glass transition temperature of the polymer [K]
T_i = temperature of the ith dynamic viscosity experiment [K]
t = polymerization time [s]
X = halogen atom/end-group functionality [−]
V = volume of the reaction system [m^3]
V_b = Le Bas molar volume [m^3 mol^{-1}]
V_A^* = the specific critical hole free volume required for a diffusional jump of A [m^3 kg^{-1}]
V_{FH} = specific hole free volume of the reaction system [m^3 kg^{-1}]
$V_{FH,A}$ = specific hole free volume of pure component A [m^3 kg^{-1}]
V_p = molar volume of the polymer [m^3 mol^{-1}]
w_B = mass fraction of the (reaction) component B [−]
x_m = (monomer) conversion [−]
x_n^{pol} = average chain length of the polymer molecules [−]

Greek Symbols

α = confidence coefficient [−]
γ = average overlap factor for the reaction system [−]
γ_A = average overlap factor for pure component A [−]
γ_0 = deformation in the linear regime [−]
$\Delta_{r,a}H^0$ = standard reaction enthalpy for the activation deactivation process [(k)J mol^{-1}]
$\Delta_{r,a}S^0$ = standard reaction entropy for the activation deactivation process [J mol^{-1} K^{-1}]
δ = delta function [−]
ϕ = Flory universal hydrodynamic constant [dL mol^{-1} cm^3]
η_A = measured dynamic viscosity of the (reaction) component A [Pa s]
$\hat{\eta}_A$ = calculated dynamic viscosity of the (reaction) component A [Pa s]
ρ = density [m^3 kg^{-1}]
σ = Lennard-Jones diameter [m]
ω = angular frequency [s^{-1}]

Subscripts

a = activation
app = apparent
calc = calculated
chem = chemical intrinsic
da = deactivation
e = end-chain (macro)radical
diff = diffusional
i, j, q = chain length (macromolecule: $i, j > 0$; initiator related $i, j = 0$; $q > 2$ (macromonomer))
is = internal standard
l = reaction step
m = monomer/midchain
$n(+1)$ = oxidation number
p = propagation
pm = propagation with macromonomer
s = solvent
t = termination
tab = tabulated

tc = termination by recombination
tot = total
y = number
0 = initial
βC = βC reaction

Superscripts

com = center-of-mass

Abbreviations

ATRP = atom transfer radical polymerization
BuA = butyl acrylate
CRP = controlled radical polymerization
CLD = chain length distribution
Cu(I)Br = copper(I) bromide
Cu(II)Br_2 = copper(II) bromide
iBoA = isobornyl acrylate
EPR = electron paramagnetic resonance
FID = flame ionization detector
FRP = free radical polymerization
GC = gas chromatography
GPC = gel permeation chromatography
MBP = methyl 2-bromopropionate
M(.)BP = initiating radical from methyl 2-bromopropionate
MMD = molar mass distribution
piBoA = poly(isobornyl acrylate)
PMDETA = N,N,N',N'',N''-pentamethyldiethylenetriamine
PLP = pulsed laser polymerization
THF = tetrahydrofuran
vol % = volume percentage
WLF = Williams−Landel−Ferry

References and Notes

(1) (a) Wang, J. S.; Matyjaszewski, K. *J. Am. Chem. Soc*. **1995**, *117*, 5614–5615. (b) Kato, M.; Kamigaito, M.; Sawamoto, M.; Higashimura, T. *Macromolecules* **1995**, *28*, 1721–1723. (c) Matyjaszewski, K.; Xia, J. *Chem. Rev*. **2001**, *101*, 2921–2990. (d) Coessens, V.; Pintauer, T.; Matyjaszewski, K. *Prog. Polym. Sci*. **2001**, *101*, 337–377. (e) Davis, K. A.; Matyjaszewski, K. *Adv. Polym. Sci*. **2002**, *159*, 1–169. (f) Wang, R.; Luo, Y. W.; Zhu, S. P. *AIChE J*. **2007**, *53*, 174.

(2) Chiefari, J.; Jeffery, J.; Mayadunne, R. T. A.; Moad, G.; Rizzardo, E.; Thang, S. H. *Macromolecules* **1999**, *32*, 7700–7702.

(3) (a) Arzamendi, G.; Plessis, C.; Leiza, J. R.; Asua, J. M. *Macromol. Theory Simul*. **2003**, *12*, 315–324. (b) Peck, A. N. F.; Hutchinson, R. A. *Macromolecules* **2004**, *37*, 5944–5951. (c) Li, D.; Grady, M. C.; Hutchinson, R. A. *Ind. Eng. Chem. Res*. **2005**, *44*, 2506–2517.

(4) Junkers, T.; Barner-Kowollik, C. *J. Polym. Sci., Part A: Polym. Chem*. **2008**, *46*, 7585–7605.

(5) Wang, W.; Nikitin, A. N.; Hutchinson, R. A. *Macromol. Rapid Commun*. **2009**, *30*, 2022–2027.

(6) Barth, J.; Buback, M. *Macromol. Rapid Commun*. **2009**, *30*, 1805–1811.

(7) Ahmad, N. M.; Charleux, B.; Farcet, C.; Ferguson, C. J; Gaynor, S. G; Hawkett, B. S; Heatly, F.; Klumperman, B.; Konkolewicz, D.; Lovell, P. A; Matyjaszewski, K.; Venkatesh, R. *Macromol. Rapid Commun*. **2009**, *30*, 2002–2021.

(8) Dervaux, B.; Junkers, T.; Baumann, M.-S.; Du Prez, F. E.; Barner-Kowollik, C. *J. Polym. Sci., Part A: Polym. Chem*. **2009**, *47*, 6641–6654.

(9) Dervaux, B.; Junkers, T.; Barner-Kowollik, C.; Du Prez, F. E. *Macromol. React. Eng*. **2009**, *3*, 529–538.

(10) Dervaux, B.; Van Camp, W.; Van Renterghem, L.; Du Prez, F. E. *J. Polym. Sci., Part A: Polym. Chem*. **2008**, *46*, 1649–1661.

(11) Coca, S.; Davis, K.; Miller, P.; Matyjaszewski, K. *Abstr. Pap. Am. Chem. Soc*. **1997**, *213*, 321-poly.

(12) Brandrup, J.; Immergut, E. H.; Grulke, E. A. *Polymer Handbook*; John Wiley and Sons: New York, 1999.

(13) (a) Coca, S.; Matyjaszewski, K. *J. Polym. Sci., Part A: Polym. Chem*. **1997**, *35*, 3595–3601. (b) Matyjaszewski, K.; Miller, P.; Fossum, E.; Nakagawa, Y. *Appl. Organomet. Chem*. **1998**, *12*, 667–673. (c) Matyjaszewski, K.; Miller, P.; Pyun, P. J.; Kickelbick, G.; Diamanti, S. *Macromolecules* **1999**, *32*, 6526–6535. (d) Matyjaszewski, K. *Polym. Int*. **2003**, *52*, 1559–1565. (e) Back, A. J.; Schork, F. J. *J. Appl. Polym. Sci*. **2006**, *103*, 819–833. (f) Jakubowski, W.; Juhari, A.; Best, A.; Koynov, K.; Pakula, T.; Matyjaszewski, K. *Polymer* **2008**, *49*, 1567–1575. (g) Seven, P.; Coshun, M.; Dimirelli, K. *React. Funct. Polym*. **2008**, *67*, 922–930.

(14) (a) Delgadillo-Velázquez, O.; Vivaldo-Lima, E.; Quintero-Ortega, I. A.; Zhu, S. *AIChE J*. **2002**, *18*, 2597–2608. (b) Wang, A. R.; Zhu, S. *Macromolecules* **2002**, *35*, 9926–9933. (c) Lutz, J. F.; Matyjaszewski, K. *J. Polym. Sci., Part A: Polym. Chem*. **2005**, *43* (4), 897–910. (d) Roa-Luna, M.; Diáz-Barber, M. P; Vivaldo-Lima, E.; Lona, L. M. F.; McManus, N. T.; Penlidis, A. *J. Macromol. Sci., Part A* **2007**, *44*, 193–203.

(15) Johnston-Hall, G.; Barner-Kowollik, C.; Monteiro, M. J. *Macromol. Theory Simul*. **2008**, *17*, 460–469.

(16) Barner-Kowollik, C.; Russell, G. T. *Prog. Polym. Sci*. **2009**, *34*, 1211–1259.

(17) D'hooge, D. R.; Reyniers, M.-F.; Marin, G. B. *Macromol. React. Eng*. **2009**, *3*, 185–209.

(18) (a) Vrentas, J. S.; Duda, J. L. *J. Polym. Sci., Part B: Polym. Phys*. **1977**, *15*, 403–416. (b) Vrentas, J. S.; Duda, J. L. *J. Polym. Sci., Part B: Polym. Phys*. **1977**, *15*, 417–439. (c) Vrentas, J. S.; Duda, J. L.; Ling, H.-C. *J. Polym. Sci., Part B: Polym. Phys*. **1984**, *22*, 459–469. (d) Vrentas, J. S.; Vrentas, C. M. *J. Polym. Sci., Part B: Polym. Phys*. **2003**, *41*, 501–507.

(19) Vrentas, J. S.; Vrentas, C. M. *Eur. Polym. J*. **1998**, *34*, 797–803.

(20) Faucher, S.; Okrutny, P.; Zhu, S. P. *Ind. Eng. Chem. Res*. **2007**, *46*, 2726–2734.

(21) Fu, Y.; Cunningham, M. F.; Hutchinson, R. A. *Macromol. React. Eng*. **2007**, *1*, 243–252.

(22) Dervaux, B. PhD Thesis, Ghent University, 2010.

(23) Williams, M. L.; Landel, R. F.; Ferry, J. D. *J. Am. Chem. Soc*. **1955**, *77*, 3701–3707.

(24) Stadler, F. J.; Pyckhout-Hintzen, W.; Schumers, J. M.; Fustin, C.-A.; Gohy, J.-F.; Bailly, C. *Macromolecules* **2009**, *42*, 6181–6192.

(25) Gilbert, R. G. *Pure Appl. Chem*. **1992**, *64*, 1563–1567.

(26) Wieme, J.; D'hooge, D. R.; Reyniers, M.-F.; Marin, G. B. *Macromol. React. Eng*. **2009**, *3*, 16–35.

(27) Smoluchowski, M. *Z. Phys. Chem*. **1917**, *92*, 129.

(28) Achilias, D. S. *Macromol. Theory Simul*. **2007**, *16*, 319–347.

(29) (a) Sugden, S. *J. Chem. Soc*. **1927**, 1786. (b) Biltz, W. *Raumchemie der festen Stoffe*; Voss Leipzig, 1934. (c) Haward, R. N. *J. Macromol. Sci., Rev. Macromol. Chem*. **1970**, *C4* (2), 191−241. (d) Tonge, M. P.; Gilbert, R. G. *Polymer* **2001**, *42*, 1391–1405. (e) Van Krevelen, D. W. *Properties of Polymers*; Elsevier: Amsterdam, 1997. (f) Brodkey, R. S.; Hershey, H. C. *Transport Phenonema: A Unified Approach*; McGraw-Hill: New York, 1998. (g) Zhang, X. Q; Wang, C. H. *J. Polym. Sci., Part B: Polym. Phys*. **1994**, *32*, 1951–1956. (h) Kobuchi, S.; Arai, Y. *Prog. Polym. Sci*. **2002**, *27*, 811–814. (i) Griffiths, M. C.; Strauch, J.; Monteiro, M. J.; Gilbert, R. G. *Macromolecules* **1998**, *31*, 7835–7844. (j) Achilias, D. S.; Kiparissides, C. *Macromolecules* **1992**, *24*, 3739–3750. (k) Doi, M.; Edwards, S. F. *The Theory of Polymer Dynamics*; Oxford University Press: New York, 1986. (l) Bicerano, J. *Prediction of Polymer Properties*; Marcel Dekker: New York, 1996.

(30) (a) Heuts, J. P. A.; Russell, G. T. *Eur. Polym. J*. **2006**, *42*, 3–20. (b) Heuts, J. P. A.; Russell, G. T.; Smith, G.-B. *Aust. J. Chem*. **2007**, *60*, 754–764.

(31) Johnston-Hall, G.; Monteiro, M. J. *J. Polym. Sci., Part A: Polym. Chem*. **2008**, *46*, 3155–3173.

(32) Seeliger, F.; Matyjaszewski, K. *Macromolecules* **2009**, *42*, 6050–6055.

(33) (a) Ponnuswamy, S. R.; Penlidis, A.; Kiparissides, C. *Chem. Eng. J*. **1988**, *39*, 175–183. (b) De Roo, T.; Wieme, J.; Heynderickx, G. J.; Marin, G. B. *Polymer* **2005**, *46*, 8340–8354. (c) Kwark, Y.-Y.; Novak, B. M. *Macromolecules* **2004**, *37*, 9395–9401.

(34) Nanda, A. K.; Matyjaszewski, K. *Macromolecules* **2003**, *36*, 1487–1493.

(35) Al-Harthi, M.; Soares, J. B. P; Simon, L. C. *Macromol. React. Eng*. **2007**, *4*, 468–479.

(36) Ziegler, M. J.; Matyjaszewski, K. *Macromolecules* **2001**, *34*, 415–421.

(37) Matyjaszewski, K.; Paik, H-. J.; Zhou, P.; Diamanti, S. J. *Macromolecules* **2001**, *34*, 5125–5131.

(38) Huang, J.; Pintauer, T.; Matyjaszewski, K. *J. Polym. Sci., Part A: Polym. Chem*. **2004**, *42*, 3285–3292.

(39) Junkers, T.; Theis, A.; Buback, M.; Davis, T. P.; Stenzel, M. H.; Vana, P.; Barner-Kowollik, C. *Macromolecules* **2005**, *38*, 9497–9508.

(40) Nikitin, A.; Hutchinson, R. A.; Buback, M.; Hesse, P. *Macromolecules* **2007**, *40*, 8631–8641.
(41) Hirano, T.; Yamada, B. *Polymer* **2003**, *44*, 347–354.
(42) de Kock, J. B. L.; van Herk, A. M.; German, A. L. *J. Macromol. Sci., Polym. Rev.* **2001**, *C41*, 199–252.
(43) Russell, G. T.; Napper, D. H.; Gilbert, R. G. *Macromolecules* **1988**, *21*, 2133–2140.
(44) Yurekli, Y.; Altinkaya, S. A.; Zielinski, J. M. *J. Polym. Sci., Part B: Polym. Phys.* **2007**, *45*, 1996–2006.
(45) Hong, S.-U. *Ind. Eng. Chem. Res.* **1995**, *34*, 2536–2544.
(46) (a) Levenberg, K. *Q. Appl. Math.* **1944**, *2*, 164. (b) Marquardt, D. W. *SIAM* (*Soc. Ind. Appl. Math.*) *J. Sci* **1963**, *11*, 431.
(47) (a) Vogel, H. Z. *Z. Phys.* **1921**, *22*, 645. (b) Fulcher, G. S. *J. Am. Ceram. Soc.* **1925**, *8*, 339. (c) Tammann, G.; Hesse, W. Z. *Z. Anorg. Allg. Chem.* **1926**, *156*, 245.
(48) Froment, G. F.; Hosten, L. H In Anderson, J. R., Boudart, M., Eds.; *Catalysis—Science and Technology*; Springer-Verlag: Berlin, 1981.
(49) Gallant, R. W; Yaws, C. L. *Physical Properties of Hydrocarbons*; Gulf Publishing: Houston, TX, 1993.
(50) Ferry, J. D. *Viscoelastic Properties of Polymers*; John Wiley and Sons: New York, 1980.
(51) (a) Macosko, C. W. *Principles, Measurements, and Applications* (*Advances in Interfacial Engineering*); John Wiley and Sons: New York, 1994. (b) Schwarzl, F. R. *Polymermechanik: Struktur und mechanisches Verhalten von Polymeren*; Springer-Verlag: Berlin, 1990.
(52) Sperling, L. H. *Introduction to Physical Polymer Science*; Wiley-Interscience: New York, 2001.
(53) Yamagushi, T.; Wang, B.-G.; Matsuda, E.; Suzuki, S.; Nakao, S.-I. *J. Polym. Sci., Part A: Polym. Chem.* **2003**, *41*, 1393–1400.
(54) Matyjaszewki, K.; Davis, T. P. *Handbook of Radical Polymerization*; John Wiley & Sons: Hoboken, NJ, 2002.
(55) Perry, R. H.; Green, D. W. *Perry's Chemical Engineers' Handbook*; McGraw-Hill: New York, 1998.
(56) Fischer, H. *J. Polym. Sci., Part A: Polym. Chem.* **1999**, *37*, 1885–1901.